American Journal of Botany

Botanical Society of America
leading scientists and educators
since 1893

RESEARCH ARTICLE

Fruit evolution in Hydrophyllaceae

Maria-Anna Vasile[1,4], Federico Luebert[1,2,3], Julius Jeiter[1], and Maximilian Weigend[1]

Manuscript received 19 August 2020; revision accepted 28 January 2021.

[1] Nees-Institut für Biodiversität der Pflanzen, Rheinische Friedrich-Wilhelms-Universität Bonn, Meckenheimer Allee 170, Bonn D-53115, Germany

[2] Departamento de Silvicultura y Conservación de la Naturaleza, Universidad de Chile, Santiago, Chile

[3] Universidad de Chile, Facultad de Ciencias Agronómicas, Santiago, Chile

[4] Author for correspondence (e-mail m.vasile@uni-bonn.de)

Citation: Vasile, M.-A., F. Luebert, J. Jeiter, and M. Weigend. 2021. Fruit evolution in Hydrophyllaceae. *American Journal of Botany* 108(6): 925–945.

doi:10.1002/ajb2.1691

PREMISE: Fruit type and morphology are tightly connected with angiosperm diversification. In Boraginales, the first-branching families, including Hydrophyllaceae, have one- to many-seeded capsules, whereas most of the remaining families have four-seeded indehiscent fruits. This fact argues for many-seeded capsules as the ancestral condition. However, little is known about the evolution of fruit dehiscence and seed number. The present study investigated the gynoecium and fruit development and morphology and the evolution of seed-numbers in Hydrophyllaceae.

METHODS: Gynoecium and fruit development and morphology were studied using scanning electron microscopy and x-ray microcomputed tomography. Ancestral character state reconstruction of seed number was performed using a broadly sampled phylogeny of Boraginales (*ndhF* and ITS) with an emphasis on Hydrophyllaceae.

RESULTS: Our ontogenetic studies not only demonstrate parallel developmental trajectories across Hydrophyllaceae, but also a striking diversity regarding the internal organization of the gynoecium. Ovule number appears to determine ovary structure. Many-seeded capsules are retrieved as the ancestral state of Hydrophyllaceae. At least seven transitions to fruits with (one to) four seeds and four reversals (i.e., from four- to many-seeded fruits) were reconstructed in Hydrophyllaceae.

CONCLUSIONS: Several shifts in seed number from "many" to "four" and back to "many" have taken place in capsular-fruited Hydrophyllaceae, a strikingly high number considering that seed number is virtually conserved across the rest of the order. The groups with a conserved seed number of four are characterized by indehiscent schizocarps or drupes and by seeds that are integrated into mericarps. This functional integration probably acts as an evolutionary constraint to shifts in seed number.

KEY WORDS Boraginales II; capsular fruits; dehiscent fruits; internal ovary organization; microCT; ontogeny; ovules arrangement; *Phacelia*; placentation; septa.

Fruit type is closely associated with dispersal mode (Spjut, 1994; Lorts et al., 2008), and fruit morphology and function are therefore important drivers of angiosperm diversification (Eriksson and Bremer, 1991; Bolmgren and Eriksson, 2005; Beaulieu and Donoghue, 2013). The evolution of different fruit types has been linked to habitat shifts. Thus, fleshy fruits are associated with animal dispersal in tree- and shrub-dominated habitats (Patterson and Givnish, 2002), whereas dry fruits are generally related to wind dispersal in more open, often arid habitats (Lorts et al., 2008).

Ontogenetic analyses can reveal otherwise obscured details about similarities or differences, which in turn can be key to understanding homology and/or novelty in mature forms (e.g., early vs. late sympetaly, Sher and Weber, 2009; early and late distinction of the nutlets, Luebert et al., 2016; gynobasic vs. apical style, Jeiter et al., 2018). Gynoecium structure and organization largely determine fruit shape and organization, and therefore, ontogenetic studies are essential for an understanding of fruit evolution. For example, carpel bulging, a phenomenon that has been noted for many angiosperms groups, results in the modification of ovary morphology (Endress, 2011). Several studies on fruit development in Boraginales could demonstrate that the localized expansion of the ovary walls might be a crucial step in the formation of single-seeded mericarps (Hilger, 1985, 1992; Gottschling, 2004; Gottschling et al., 2014b; Jeiter et al., 2018).

The families of Boraginales have always been defined mostly based on their divergent fruit morphology. The order falls into two major clades, Boraginales I and II, each comprising a basal grade of two small- to medium-sized families with capsular fruits (Boraginales I: Codonaceae, Wellstediaceae; Boraginales II: Hydrophyllaceae, Namaceae; Fig. 1). The remaining families of

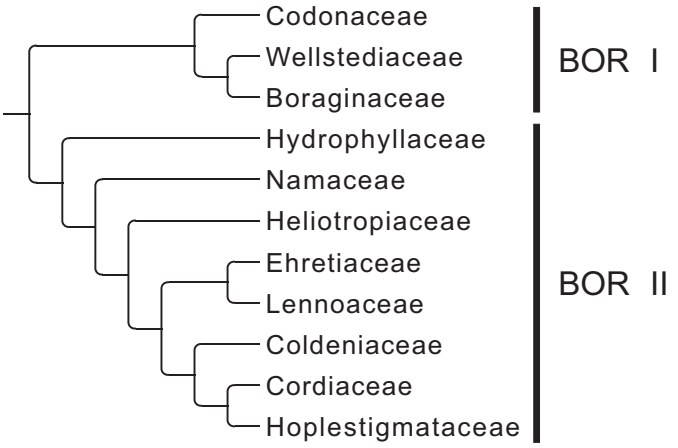

FIGURE 1. Major clades of the Boraginales. This topology is well supported based on plastid data (Weigend et al., 2014; Stull et al., 2015). BOR = Boraginales.

both clades are characterized by (mostly) four-seeded, indehiscent fruits and show higher species diversity. Their fruits usually consist of four one-seeded mericarps (nutlets) or four-seeded drupes (Weigend et al., 2014, 2016; Luebert et al., 2016; Jeiter et al., 2018). Due to the apparently convergent evolution of nutlets in both major clades, gynoecium and fruit development and evolution have been addressed in several studies (Hilger, 1985, 1992; Hofmann, 1999; Gottschling et al., 2014a, 2014b; Jeiter et al., 2016, 2018). Based on recent molecular phylogenies and morphological evidence, capsular fruits are plausibly the plesiomorphic condition of both clades (Weigend et al., 2014; Luebert et al., 2016; Zhang et al., 2020). However, ancestral character state reconstructions for Boraginales fruits and studies on gynoecium ontogeny are still lacking in the literature.

Hydrophyllaceae and Namaceae (Boraginales II) are characterized by four- to pluri-ovulate ovaries developing into one- to many-seeded capsules (Luebert et al., 2016). The remaining clades of Boraginales II have drupes or nutlets, with the only exception of Lennoaceae, a family of parasitic plants with secondary multiplication and subdivision of the carpels as a clearly derived condition (Yatskievych and Mason, 1986). Reduction of ovule number and mericarp formation in Boraginales II, originating from an ancestor with many-seeded capsular fruits, seems to be the most likely explanation for this phylogenetic pattern, but the evolution of distinct morphological traits underlying the transition from capsules to nutlets is still poorly understood.

Hydrophyllaceae comprise approximately 240–260 species in 12 genera (Hofmann et al., 2016; Luebert et al., 2016), five of which are monotypic and the rest include two to nine species. *Phacelia* Juss. is the largest and most diverse genus, comprising more than three fourths of the species in the family (ca. 207 spp.; Hofmann et al., 2016). Hydrophyllaceae are characterized by a syncarpous, bicarpellate, superior to semi-inferior gynoecium usually with a basal gynoecial nectary disc (Hofmann et al., 2016; Jeiter and Weigend, 2018). All Hydrophyllaceae have capsular fruits (Fig. 2), but there is considerable diversity with regards to internal ovary organization with differences in placentation and divergent ovule and seed numbers (Brand, 1913; Atwood, 1975; Chuang and Constance, 1992; Jepson and Hickman, 1993; Walden and Patterson, 2012). The usually intrusive parietal placentae and the development of false septa (partitions in the ovary independent of the carpel margins) can lead to 2- to 4-locular ovaries. Dehiscence tissue in all Hydrophyllaceae originates in the median carpel plane and the small false septa (Hofmann et al., 2016). Few ontogenetic studies have been

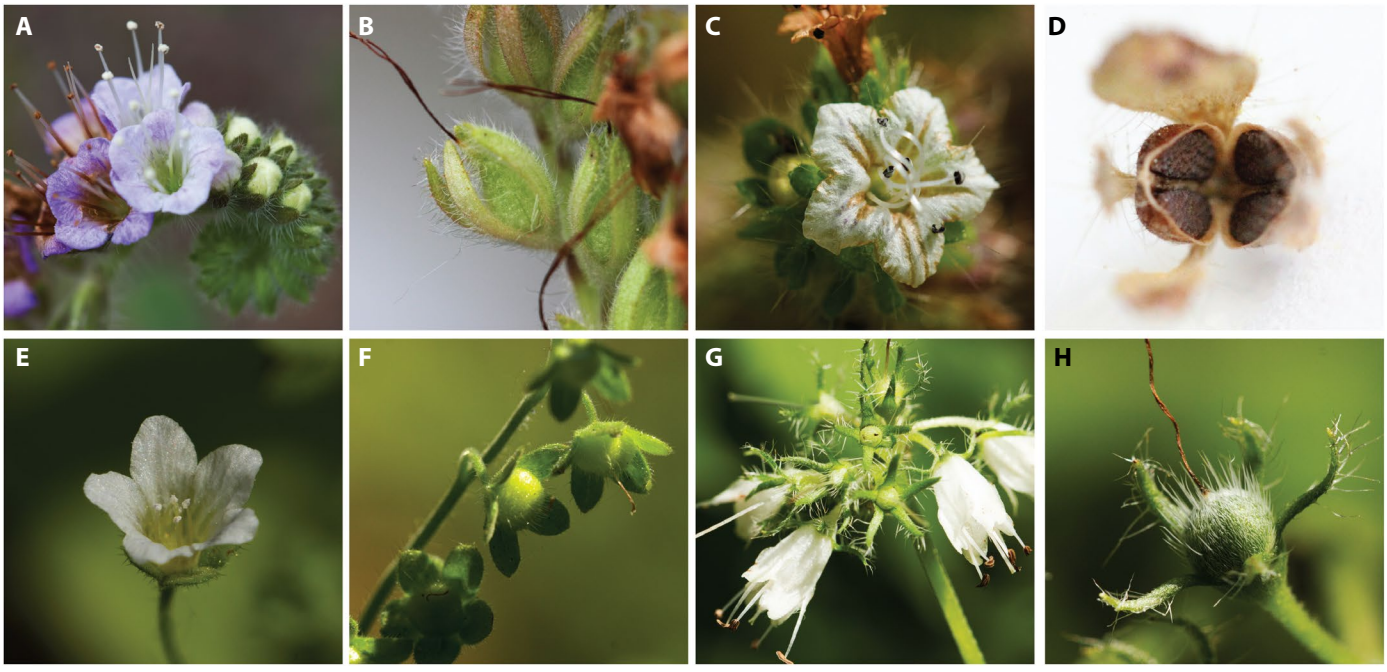

FIGURE 2. Flowers and fruits of Hydrophyllaceae. (A, B) *Phacelia secunda*. (A) Inflorescence. (B) Infructescence with immature capsules. (C, D) *Phacelia malvifolia*. (C) Anthetic flower. (D) Opened capsule with four seeds. (E, F) *Eucrypta chrysanthemifolia*. (E) Anthetic flower. (F) Infructescence with immature capsules. (G, H) *Hydrophyllum virginianum*. (G) Inflorescence with some young fruits. (H) Close-up of an immature capsule.

published on Hydrophyllaceae (Payer, 1857; Berg, 1985; Di Fulvio et al., 1999; Hofmann, 1999). In broad taxonomic studies (Brand, 1913; Hofmann et al., 2016), outer and inner gynoecium morphology, ovule number, seed shape, and surface morphology have been used as diagnostic characters, but comparative ontogenetic studies are required for an understanding of the evolutionary processes.

This study addresses the following questions: (1) How does gynoecium and fruit development vary across the Hydrophyllaceae? (2) Are many-seeded capsules the ancestral condition of Hydrophyllaceae? (3) Does the shift/do the shifts in seed number in Hydrophyllaceae reflect a phylogenetic pattern? To this end, we compiled data on seed number from the literature and added new morphological and developmental data based on scanning electron microscopy (SEM) and microcomputed tomography (μCT). We finally inferred an ancestral character state reconstruction for Boraginales with a large sampling within Hydrophyllaceae.

MATERIALS AND METHODS

Plant material for morphological analysis

Fresh flowers in different developmental stages and immature and mature fruits were either obtained from Bonn University Botanic Garden or sampled during field trips (Table 1). Gynoecium and fruit development were studied with SEM and μCT, but in a few cases only specific developmental stages could be studied (e.g., *P. viscosa*; Table 1). Samples were fixed in formaldehyde–acetic acid–ethanol (FAA; formaldehyde 4%, acetic acid 4%, ethanol 70%) for at least 1 week. After fixation, samples were either stored in FAA or ethanol (70%).

Scanning electron microscopy (SEM)

Subsets of samples were transferred into ethanol (70%). Ethanol was exchanged three times at 15-min intervals. The samples were then dissected using a stereomicroscope and transferred to ethanol (70%) for storage. For chemical dehydration, the samples were stored overnight in ethanol (70%) and acetic acid (4%) before being transferred into 100% formaldehyde dimethyl acetal (FDA) for 2 h, then into FDA–acetone (1:1) for 1 h, and then acetone (100%). Acetone was exchanged three times at 60-min intervals. Samples were finally stored in acetone (100%). The dehydrated material was dried in a critical-point dryer (CPD 020, Balzers Union, Liechtenstein) following standard protocol. Dried specimens were mounted on glass slides on aluminum stubs using conductive carbon cement (Leit-C, PLANO, Wetzlar, Germany). The mounted samples were further dissected under the stereomicroscope and subsequently sputter-coated with gold or palladium in a sputter-coater (SCD 040, Balzers Union, Liechtenstein) for 1.5 to 3 min (according to the specimen complexity) at ~30 mA. Images were obtained using a Stereoscan 200 electron microscope (Cambridge, Cambridge, UK) at 15 kV. Contrast and brightness of the images were improved using standard image-editing software (e.g., Photoshop CS6, Adobe, San Jose, CA, USA).

X-ray microcomputed tomography

For x-ray microcomputed tomography (μCT), FAA-fixed samples were transferred into an infiltration medium consisting of 70% ethanol plus 1% w/v phosphotungstic acid (PTA) for at least 2 weeks to improve their contrast (Staedler et al., 2013). The infiltration medium was exchanged every second day. After infiltration, samples were dehydrated in graded ethanol series (85%, 96%, 99%) plus 1% w/v PTA and, finally, acetone (100%) plus 1% PTA. The dehydrated samples were critical-point dried (CPD 020, Balzers Union). Specimens were mounted on thin aluminum rods using two-component epoxy glue (UHU PLUS Sofortfest, UHU, Bühl, Germany).

Scans were performed in a SkyScan 1272 (Bruker Co., Billerica, MA, USA) equipped with a Hamamatsu L11871-20 source (Hamamatsu Photonics, Hamamatsu, Japan) and a Ximea xiRAY16 camera (Ximea GmbH, Münster, Germany). A 3D reconstruction from the scanning data was performed using the InstaRecon Engine v2 (InstaRecon, Champaign, IL, USA). Some scans were performed in Vienna on a MicroXCT-200 imaging system (XRadia, Pleasanton, CA, USA) with a L9421-02 90kV Microfocus X-ray source (Hamamatsu Photonics, Iwata City, Japan), and the 3D reconstruction was performed using XMReconstructor 8.1.6599 (XRadia). Scan settings are given in Appendix S1. The resulting image stacks were initially processed using the ImageJ distribution Fiji (Schindelin et al., 2012) for cropping and reducing the number of colors from 16- to 8-bits. The edited image stacks were visualized with Amira 6.5 (Thermo Fisher Scientific, Waltham, MA, USA) using the Volren function. Volume was edited to remove flower or fruit parts not relevant for our study (e.g., sepals and trichomes) using the Volume Edit function. Virtual cross and longitudinal sections through the data set were created using the Slice function. The histogram was manually adjusted between 5000 and 40,000 at 16-bits and 25 and 200 at 8-bits.

Taxon sampling

Phylogenetic data based on two markers—chloroplast NADH dehydrogenase F (*ndhF*) and nuclear internal transcribed spacer (ITS)—are from Vasile et al. (2020) and have been analyzed seperately. They include representatives from all families of Boraginales, except for Lennoaceae (where all NADH dehydrogenase [*ndh*] genes are absent; Schneider et al., 2018). Hydrophyllaceae and Namaceae were extensively sampled. Outgroup taxa include representatives of Gentianales, which is likely the sister order to Boraginales (Stull et al., 2015; Zhang et al., 2020). Information regarding names, voucher specimens and GenBank accessions can be found in Appendix S2.

Ancestral character state reconstruction

A matrix with seed number as a proxy of ovule number for all Boraginales taxa included in our analysis was created based on a literature search (Appendix S3). Ovule number was used whenever available. Since seed number is sometimes the result of the lack of fertilization or the abortion of fertilized ovules, it does not always reflect a structural feature of the fruit. The minimum number of ovules found in Hydrophyllaceae is four, but sometimes only a single seed develops. Conversely, seed number is not fixed in pluriovulate/many-seeded species, where the number of seeds in mature fruits may vary, e.g., from 30 to 60 in *Phacelia bolanderi* A.Gray, from 10 to 40 in *Phacelia divaricata* (Benth.) A.Gray or from 50 to 200 in *Phacelia perityloides* Coville. Therefore, seed number was coded as a binary character for the analysis: (1) species with one

TABLE 1. Studied taxa and vouchers.

Taxon [Section]	Gynoecium development (SEM)	Gynoecium development (µCT)	Fruit development (SEM)	Anthetic flower (µCT)	Mature capsule (µCT)	Mature capsule (SEM)	Seeds (SEM)	Ovule number	Voucher	Herbarium
Draperia systyla (A.Gray) Torr.	+		+	+		+	+	4	US-0-BONN-38920	BONN
Eucrypta chrysanthemifolia (Benth.) Greene	+		+	+		+	+	8	US-0-BONN-36929	BONN
Hydrophyllum virginianum L.	+		+	+		+	+	4	xx-0-BONN-36861	BONN
Nemophila menziesii Hook. & Arn.	+		+	+		+	+	ca. 12	xx-0-BONN-38177	BONN
Phacelia egena (Brand) Greene ex J.T.Howell [sect. *Phacelia*]		+		+	+			4	US-0-BONN-37009	BONN
Phacelia campanularia A.Gray [sect. *Whitlavia*]	+	+	+	+	+	+	+	ca. 80	PE-0-BONN-35820	BONN
Phacelia cumingii (Benth.) A.Gray [sect. *Euglypta*]		+		+	+	+	+	ca. 24	Luebert & Böhnert 3696	BONN
Phacelia malvifolia Cham. [sect. Ramosissimae]		+		+	+			4	US-0-BONN-37883	BONN
Phacelia secunda J.F.Gmel. [sect. *Phacelia*]		+		+	+			4	CL-0-BONN-38409	BONN
Phacelia setigera Phil. [sect. *Glandulosae*]		+		+	+			4	Moreira & Luebert 2440	BONN
Phacelia tanacetifolia Benth. [sect. *Ramosissimae*]	+	+	+	+	+	+	+	4	xx-0-BONN-31966	BONN
Phacelia viscosa Phil. [sect. *Glandulosae*]				+		+	+	4	Luebert & Böhnert 3640	BONN

to four seeds, (2) species with more than four seeds. The former corresponds to fruits originating from a four-ovulate ovary with ovules always arranged in one layer, while the latter originates from a pluri-ovulate ovary with ovules arranged in several layers, which is confirmed by our ontogenetic results presented below. This coding accounts for the two major groups of fruits found in Boraginales in general: fruits with four (or less) seeds and many-seeded fruits. Ancestral character state reconstruction of the seed number was then performed independently for ITS and *ndhF*, using the R packages ape (Paradis and Schliep, 2019) and phytools (Revell, 2012). To simulate a stochastic character map on the ML phylogenetic trees, we implemented the function make.simmap with 1000 simulations and parameters: Q= "mcmc" and pi= "estimated".

Plotting seed number range

The same matrix (Appendix S3) was used to plot the seed number ranges across Hydrophyllaceae. The use of literature data and the divergent reported seed number for the same species in a few cases, introduce some uncertainty. However, this data set was sufficient for visualizing seed number ranges.

RESULTS

Gynoecium development up to anthesis: SEM-data

The external morphology of the gynoecium across Hydrophyllaceae from early developmental stages to the anthetic flower in six species is shown in Figs. 3 and 4. The two independent carpels are the last organs to be initiated in the center of the flower. Shortly after their emergence, they fuse and develop into a gynoecial cone (Figs. 3A, 3E, 4A, 4I, 4M). After forming of the gynoecial cone, the gynoecium differentiates into an ovary, a bifid style with two separate stigmas and a nectary disc at the base of the ovary. Ovary position varies from superior in *Draperia systyla*, *Eucrypta chrysanthemifolia*, and all eight *Phacelia* species studied

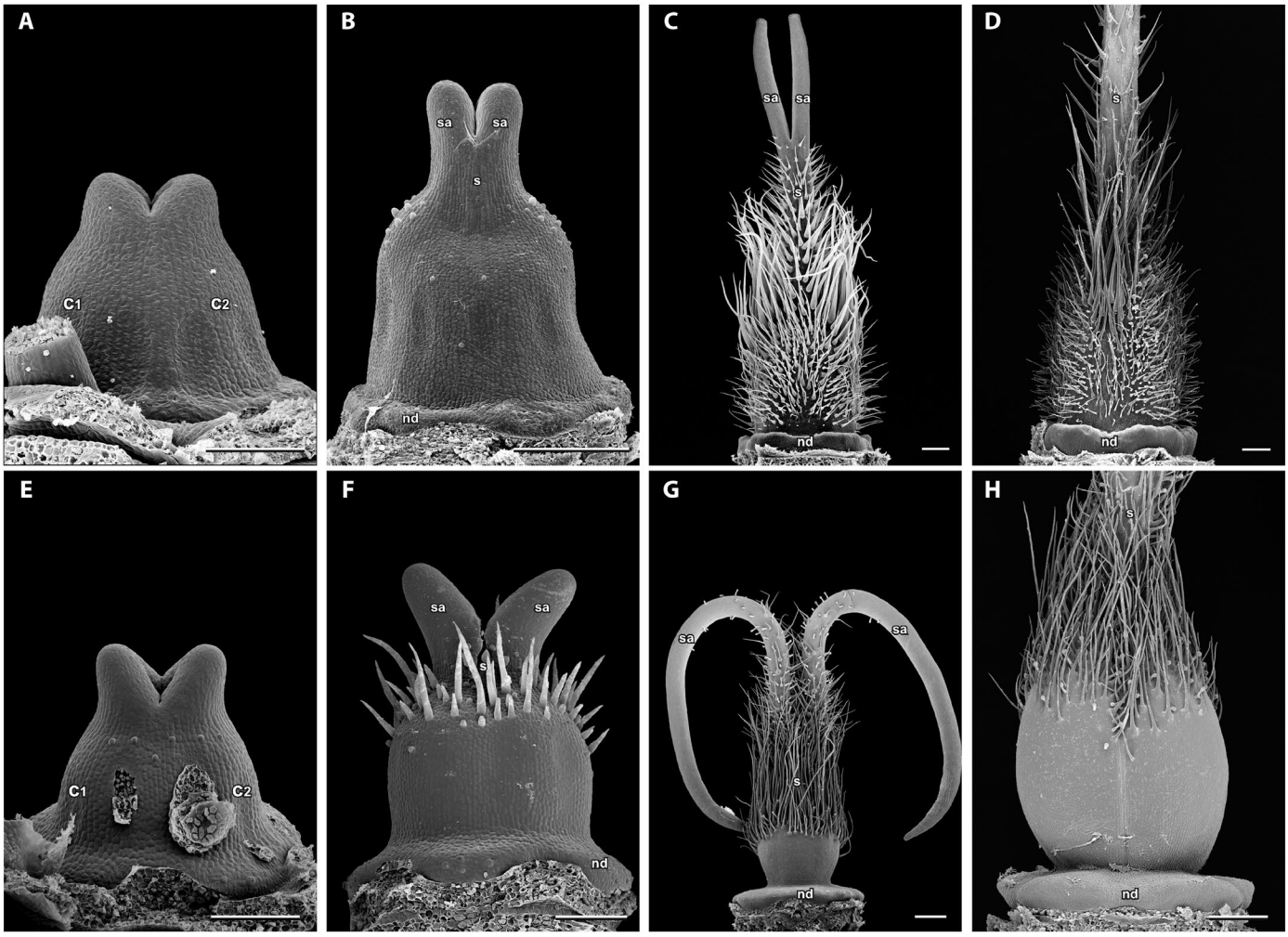

FIGURE 3. Gynoecium development in two species of *Phacelia*; lateral view (looking at the line of carpel fusion). (A–D) *Phacelia campanularia*. (A) Gynoecial cone. (B) Onset of the ovary formation. (C) Enlargement of the ovary and the flattened nectary disc, elongation of the stylodia, development of the papillate stigmatic surface. (D) Gynoecium at anthesis; close-up of the ovary. (E–H) *Phacelia tanacetifolia*. (E) Gynoecial cone. (F) Onset of the ovary formation. (G) Enlargement of the ovary and the flattened nectary disc, elongation of the stylodia, development of the papillate stigmatic surface. (H) Gynoecium at anthesis; close-up of the ovary. c1, carpel 1; c2, carpel 2; nd, nectary disc; s, style; sa, stylodia. Bars (A, E, F) = 100 μm; (B–D, G, H) = 500 μm.

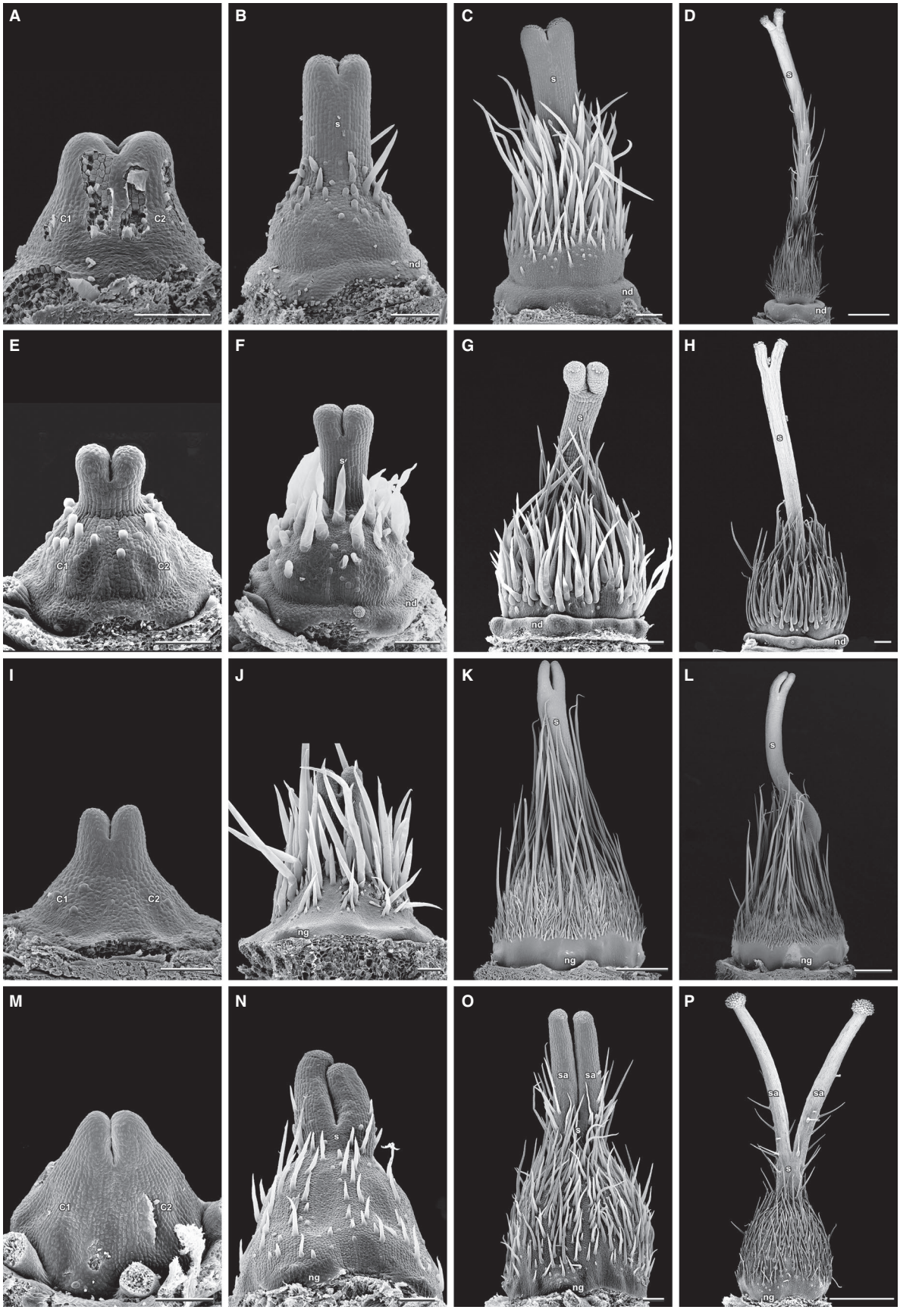
A
C1
C2
B
s
nd
C
s
nd
D
s
nd
E
C1
C2
F
s
nd
G
s
nd
H
s
nd
I
C1
C2
J
ng
K
s
ng
L
s
ng
M
C1
C2
N
s
ng
O
sa
sa
s
ng
P
sa
sa
s
ng

FIGURE 4. Gynoecium development in *Draperia*, *Eucrypta*, *Hydrophyllum*, and *Nemophila*; lateral view (looking at the line of carpel fusion). (A–D) *Draperia systyla*. (A) Gynoecial cone. (B) Ovary formation. (C) Enlargement of the ovary, elongation of the style, development of the stigmatic papillae and of the nectary disc. (D) Anthetic gynoecium. (E–H) *Eucrypta chrysanthemifolia*. (E) Ovary formation shortly after the gynoecial cone stage. (F, G) Enlargement of the ovary, elongation of the style, development of the stigmatic papillae and of the nectary disc. (H) Anthetic gynoecium. (I–L) *Hydrophyllum virginianum*. (I) Gynoecial cone. (J) Ovary formation. (K) Enlargement of the ovary, elongation of the style, development of the stigmatic papillae and of the nectary glands. (L) Gynoecium shortly before anthesis; the ovary has reached its final size, but the style will continue to elongate. (M–P) *Nemophila menziesii*. (M) Gynoecial cone. (N) Ovary formation. (O) Enlargement of the ovary, elongation of the stylodia, development of the stigmatic papillae and of the nectary glands. (P) Anthetic gynoecium with distinct stigmatic heads. c1, carpel 1; c2, carpel 2; nd, nectary disc; ng, nectary glands; s, style; sa, stylodia. Bars (A–C, E–H, I, J, M–O) = 100 μm; (D, K, L, P) = 500 μm.

here, to semi-inferior in *Nemophila menziesii* and *Hydrophyllum virginianum*. Comparative morphological characterization of the mature forms of the studied taxa is summarized in Table 2.

Phacelia campanularia (Fig. 3A–D)—The ovary and the nectary disc start to shape very early, before the gynoecial cone is completely closed (Fig. 3A). When the gynoecial cone closes, the nectary disc develops with five lobes in antepetalous position at the base of the ovary (Fig. 3B, C). At anthesis, the circumference of the nectary disc slightly exceeds that of the ovary (Fig. 3D). The apical part of the cone develops into a style (Fig. 3B). The papillate stigmatic surface develops on the tips of the two stylar branches at intermediate developmental stages (Fig. 3C).

Phacelia tanacetifolia (Fig. 3E–H)—The ovary and the nectary disc initiate before the gynoecial cone is completely closed. After the gynoecial cone closes, the nectary disc gradually flattens, and its diameter significantly exceeds the diameter of the ovary at anthesis (Fig. 3G, H). The two deeply bifurcate stylar branches emerging from the style, bend to opposite directions during gynoecium development and become erect at anthesis (Fig. 3F, G). The stigmatic surface is restricted to a small tip.

Draperia systyla (Fig. 4A–D)—A conical ovary is formed after the closing of the gynoecial cone. Its base develops into a nectary disc, with five large antepetalous lobes covered with nectarostomata (Fig. 4C, D). The circumference of the nectary disc slightly exceeds that of the ovary at anthesis (Fig. 4D). After the style starts to form, the stigmatic papillae are initiated (Fig. 4B).

Eucrypta chrysanthemifolia (Fig. 4E–H)—After the gynoecial cone closes, a conical ovary is formed (Fig. 4E). The nectary disc has five small lobes with only a few nectarostomata and barely exceeds the circumference of the ovary (Fig. 4G, H). The stigmatic papillae are initiated together with the initiation of the style formation (Fig. 4E).

Hydrophyllum virginianum (Fig. 4I–L)—The ovary is conical at the onset of development. Its base develops into a flat nectary disc, which has five distinct nectary lobes (Fig. 4I, J). As the ovary enlarges, the nectary disc does not appear as a separate disc. At anthesis, the nectary disc is distinguishable only by the presence of five separate glands surrounding the base of the ovary (Fig. 4K, L). The apical part of the gynoecial cone develops into two short stigmatic lobes (Fig. 4I), which gradually elongates into a single style (Fig. 4J, K). The stigmatic surface develops from intermediate developmental stages to anthesis (Fig. 4J–L).

Nemophila menziesii (Fig. 4M–P)—After closing of the gynoecial cone, a conical ovary is formed (Fig. 4M). Five separate nectary glands develop at the lower part of the ovary shortly after gynoecial cone formation (Fig. 4M–O). The apical part of the gynoecial cone develops into a short style with two long stylar branches (Fig. 4M, N). The papillate stigmatic surface starts to develop in intermediate developmental stages (Fig. 4N, O). At anthesis, each style branch has a distinct subglobose stigmatic head with a sharp, papillate receptive surface (Fig. 4P).

Gynoecium development up to anthesis: μCT-data

Of the eight *Phacelia* species scanned with μCT, six species were four-ovulate, and two species were pluri-ovulate. The early gynoecium development in the four-ovulate species was almost identical. Initiation of the four ovules takes place at the same developmental stage. Minor differences regarding placental bundles and ovules shape and size become distinct in later developmental stages. The two intrusive placentae with false septa usually create two compartments in the ovary. A compitum is formed when the gynoecium closes. As the gynoecium develops, each style branch has a pollen tube transmitting tissue, and they are both connected through a very short compitum. In the following text, the results of *P. malvifolia* (Fig. 5A–L) as an example for a four-ovulate species and *P. campanularia* (Fig. 6A–L) and *P. cumingii* (Fig. 7A–L) as examples for pluri-ovulate species are described in detail. The anthetic gynoecia of the remaining studied taxa are briefly described. Comparative morphological characterization for the internal ovary organization can be found in Table 2.

Phacelia malvifolia (Figs. 5A–L, 8K, 8L)—During early gynoecium development, the septa are initiated as erected ridges (Fig. 5B). Then, the parietal placentation develops by contraction of the septa to the periphery (Fig. 5D), and four ovules are initiated (Fig. 5C). The ovules appear in the medial domain before the gynoecial cone is completely closed (Fig. 5C, D), and they become distinct when the cone is finally closed (Fig. 5E, F). The two parietal placentae gradually enlarge and become discernible (Fig. 5G, H). During the preanthetic developmental stages after closing of the gynoecial cone, ovary size increases, placentae and ovules develop, and vascular organization in the placentae is formed (Fig. 5E–H). Once all parts of the gynoecium are differentiated, the nectary disc enlarges up to anthesis (Fig. 5F, H, J). The ovary locules slightly intrude into the level of the nectary disc. At anthesis, the four ovules (two per placenta) are arranged in one level (Fig. 5I, J). Ovules are epitropous-ventral (the micropyle points distally; the raphe points toward the central ovary axis). A basal and an apical septum are visible (continuation of the stylar canal; Fig. 5J).

Phacelia campanularia (Figs. 6A–L, 8O, 8P)—In this pluri-ovulate species, the developmental gap between the successive flowers of

TABLE 2. Summary of different morphological characters accross Hydrophyllaceae.

Taxon	ON	Seed number	OP	Ovary position	Ovary form	Nectar disc	Style	Placentation	Length/size of placenta	Size of septa	Ovary locules	Number of ovule layers	ON per placenta	ON per layer
Draperia systyla	4	1 to 4	EV	S	Ovoid	Distinct	Style-cleft close to stigmatic heads	Intrusive parietal	Short/ small	Long	2	1	2	4
Eucrypta chrysanthemifolia	8	≤ 8	EV	S	Globose	Distinct	Style-cleft close to stigmatic heads	Intrusive parietal	Fills the ovary/ large and flattened	Very short	5	1	4	8
Hydrophyllum virginianum	4	2	PV	SI	Conical	Absent (nectary glands present)	Style-cleft close to stigmatic heads	Intrusive parietal	Fills the ovary/ large	Very short	2	1	2	4
Nemophila menziesii	12	≤ 12	PV	SI	Ovoid	Absent (nectary glands present)	Deeply bifurcate	Intrusive parietal	Long/ large	Very short	1	3	6	4
Phacelia egena [sect. *Phacelia*]	4	(1 to) 4	EV	S	Globose to ovoid	Distinct	Bifid	Intrusive parietal	Short/ small to medium	Medium to long	2	1	2	4
Phacelia campanularia [sect. *Whitlavia*]	ca. 80	≤ 80	EV	S	Conical to ovoid	Distinct	Bifid	Intrusive parietal	Long/ large	Medium to long	2	9 to 10	ca. 40	(4 to) 8
Phacelia cumingii [sect. *Euglypta*]	24 to 28	≤ 28	PV	S	Conical to ovoid	Distinct	Style-cleft close to stigmatic heads	Intrusive parietal	Long/ large	Medium to long	2	6 to 7	12 to 14	4
Phacelia malvifolia [sect. Ramosissimae]	4	(1 to) 4	EV	S	Ovoid	Distinct	Deeply bifurcate	Intrusive parietal	Medium/ medium	Medium	2	1	2	4
Phacelia secunda [sect. *Phacelia*]	4	(1 to) 4	EV	S	Globose to ovoid	Distinct	Bifid	Intrusive parietal	Medium/ medium	Medium to long	2	1	2	4
Phacelia setigera [sect. *Glandulosae*]	4	(1 to) 4	EV	S	Ovoid	Distinct	Deeply bifurcate	Intrusive parietal	Medium/ large	Short to medium	2	1	2	4
Phacelia tanacetifolia [sect. *Ramosissimae*]	4	(1 to) 4	EV	S	Ovoid	Distinct	Deeply bifurcate	Intrusive parietal	Medium/ medium	Medium	2	1	2	4
Phacelia viscosa [sect. *Glandulosae*]	4	(1 to) 4	EV	S	Ovoid	Distinct	Deeply bifurcate	Intrusive parietal	Medium/ large	Short to medium	2	1	2	4

Notes: ON = ovule number, OP = ovule position, EV = epitropous-ventral, PV = pleurotropous-ventral, S = superior, SI = semi-inferior

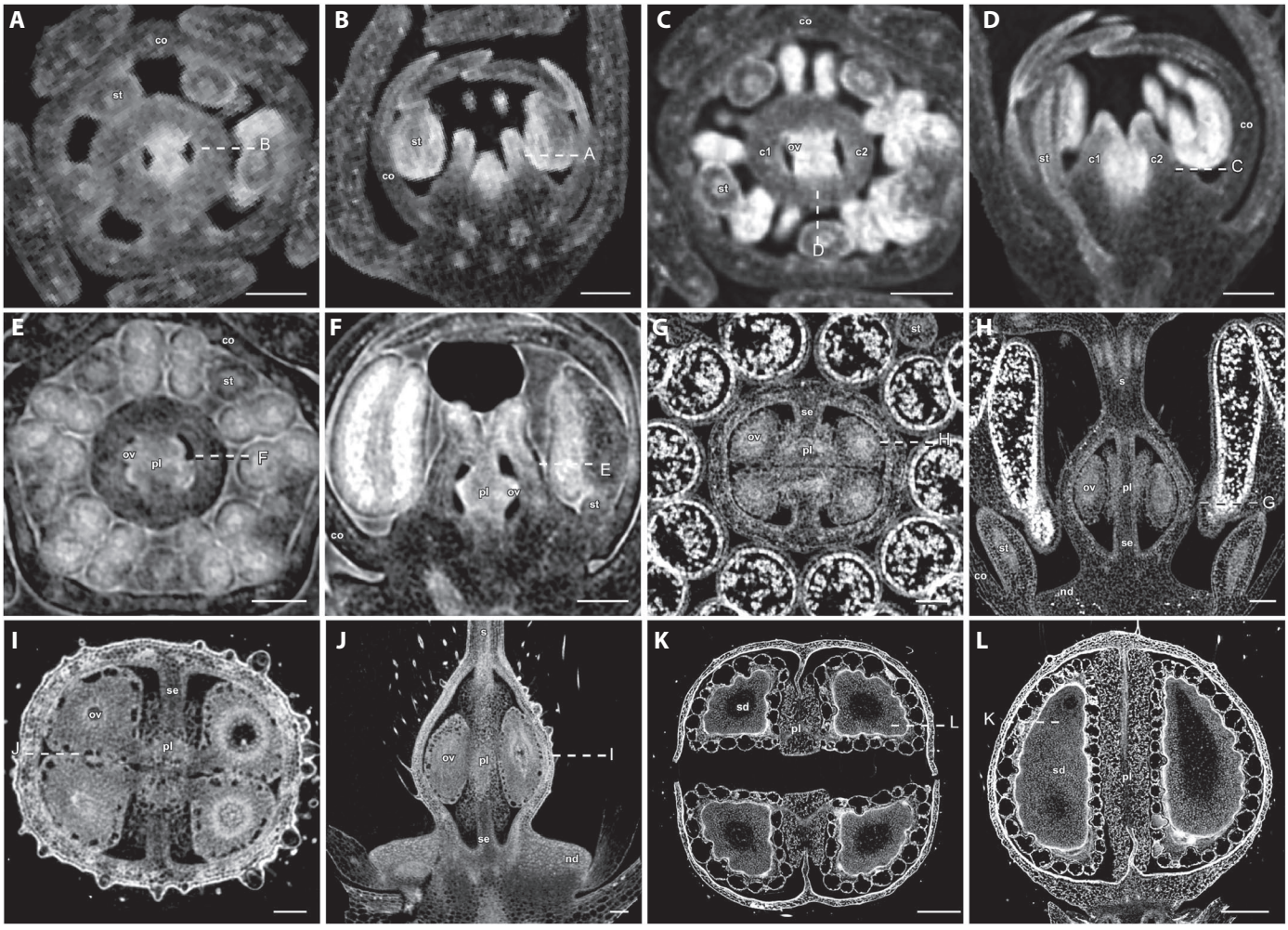

FIGURE 5. Internal development of the gynoecium and fruit in *Phacelia malvifolia* based on virtual sections reconstructed from µCT scans. (A, B) Young flower with gynoecium before gynoecial cone formation. (A) Virtual cross section. (B) Virtual longitudinal section. (C–F) Young flowers with gynoecium at the stage of gynoecial cone; onset of ovule development. (C, E) Virtual cross section. (D, F) Virtual longitudinal section. (G, H) Pre-anthetic flower focused on the gynoecium. (G) Virtual cross section. (H) Virtual longitudinal section. (I, J) Anthetic gynoecium. (I) Virtual cross section through the ovary, mid level. (J) Virtual longitudinal section through the ovary, within the carpels. (K, L) Mature capsule. (K) Virtual cross section through the mature capsule, mid level. (L) Virtual longitudinal section through the mature capsule. Dashed white lines with letters indicate the corresponding reconstructed sections in other panels of this figure. c1, carpel 1; c2, carpel 2; co, corolla; nd, nectary disc; ov, ovule; pl, placenta; s, style; sd, seed; se, septa; st, stamen. Bars (A–J) = 100 µm; (K–L) = 500 µm.

the same inflorescence was significant, at least in young flowers. After the gynoecial cone closes, the septa and the ovules are already clearly differentiated (Fig. 6A, B). The ovules develop in an acropetal sequence (Fig. 6B, D, F). Each placenta has four rows of ovules (Fig. 6C, E, G, I) and, in total, about 40 ovules per placenta at anthesis (Fig. 6I, J), arranged in several layers. In each individual carpel, the ovules alternate (Fig. 8P). Toward the style and toward the base of the ovary, the number of ovules is reduced due to the smaller diameter of the ovary (Fig. 8P).

Phacelia cumingii (Figs. 7A–L, 8M, 8N)—A clear developmental gap between the successive flowers of the same inflorescence, especially in the young developmental stages, was observed. The initiation of ovules is visible when the gynoecial cone closes (Fig. 7A, B). The ovules develop in an acropetal sequence. The ovules are arranged in two rows per placenta (Fig. 7I, J). Style and compitum develop late (Fig. 7F). The elongation of the septa up to anthesis is significant (Fig. 7C–J). At anthesis, there are about 14 ovules per placenta and 28 ovules in total (Fig. 7J), arranged in many layers. The two rows of ovules in an individual carpel alternate. Ovules are pleurotropous-ventral (the micropyle points to the side).

Anthetic gynoecia across Hydrophyllaceae—The anthetic gynoecia of all eight *Phacelia* species and the other four representatives of Hydrophyllaceae (*Draperia systyla*, *Eucrypta chrysanthemifolia*, *Hydrophyllum virginianum*, and *Nemophila menziesii*) are shown in Figs. 8 and 9, respectively (see also Table 2).

Phacelia secunda (Fig. 8A, B) and *P. egena* (Fig. 8C, D) have almost identical internal morphology. *Phacelia secunda* has a slightly different ovule shape, and the two locules extend down to the level of the nectary disc. The shape and the internal architecture of the ovary of *P. viscosa* (Fig. 8E, F) resemble that of *P. setigera* (Fig. 8G,

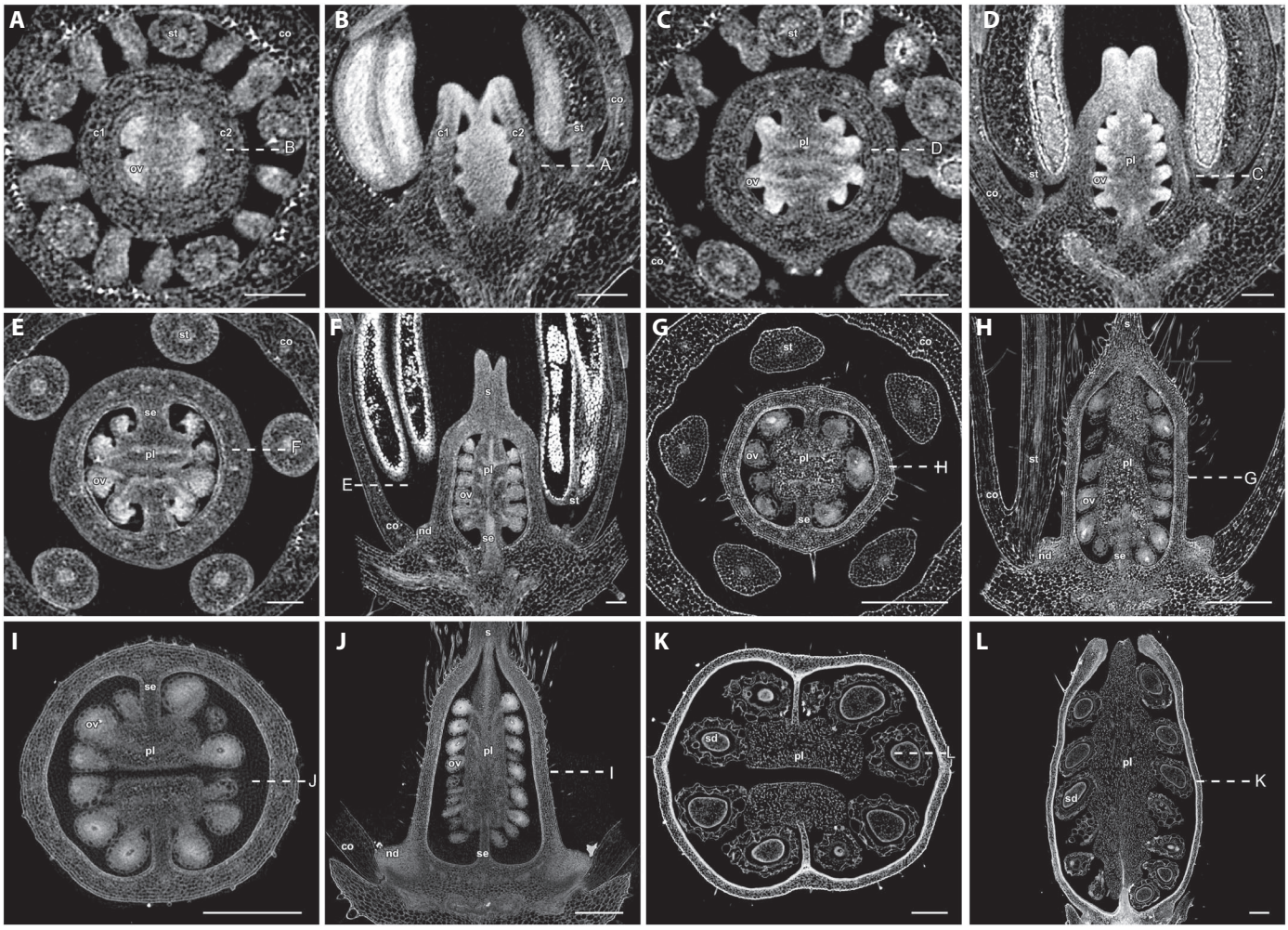

FIGURE 6. Internal development of the gynoecium and fruit in *Phacelia campanularia* based on virtual sections reconstructed from µCT scans. (A, B) Young flower with gynoecium at the stage of gynoecial cone; onset of ovules development. (A) Virtual cross section. (B) Virtual longitudinal section. (C, D) Young flowers with gynoecium at the stage of ovary formation; individual ovules become distinct. (C) Virtual cross section. (D) Virtual longitudinal section. (E–H) Pre-anthetic flowers focused on the gynoecium; ovary enlargement, style elongation, further development of ovules and placentae, development of distinct septa. (E, G) Virtual cross section. (F, H) Virtual longitudinal section. (I, J) Anthetic gynoecium. (I) Virtual cross section through the ovary, mid level. (J) Virtual longitudinal section through the ovary, within the carpels. (K, L) Mature capsule. (K) Virtual cross section through the mature capsule, mid level. (L) Virtual longitudinal section through the mature capsule. Dashed white lines with letters indicate the corresponding reconstructed sections in other panels of this figure. c1, carpel 1; c2, carpel 2; co, corolla; nd, nectary disc; ov, ovule; pl, placenta; s, style; sd, seed; se, septa; st, stamen. Bars (A–F) = 100 µm; (G–L) = 500 µm.

H). The ovary locules extend into the level of the nectary disc for both species. The ovules of *P. setigera* differ slightly in shape and are cymbiform to ovate. The anthetic gynoecium of *P. tanacetifolia* (Fig. 8I, J) is similar to that of *P. malvifolia* (Figs. 5I, 5J, 8K, 8L). The ovules of *P. tanacetifolia* occupy almost the entire volume of each locule. Their outer integument touches the ovary wall and the adjacent ovule (Fig. 8I, J).

The internal gynoecium organization of *Draperia systyla* (Fig. 9A, B) resembles that of the four-ovulate *Phacelia* species. Each parietal placenta bears two ovoid ovules. There are very long basal septa and short apical ones, and the placental tissue is short and close to the apical septa (Fig. 9B). Thus, in a cross section (Fig. 9A) at the mid level of the ovary, the placenta bundles are barely visible. The ovary locules distinctly extend to the level of the large nectary disc (Fig. 9B).

Eucrypta chrysanthemifolia (Fig. 9C, D) has a considerably different internal ovary organization. The two large and very flattened intrusive parietal placentae divide the ovary into five compartments (Fig. 9C), and the ovoid ovules, four per placenta, develop on the inner and outer surfaces of the placentae (Fig. 9C, D). The eight ovules are arranged in one layer. In the central compartment, the ovules of the two placentae alternate due to lack of space (Fig. 9C, D). The nectary tissue consists of a few layers (Fig. 9D).

In *Hydrophyllum virginianum* (Fig. 9E, F), the spatial arrangement of ovules resembles more that of *E. chrysanthemifolia*, than those of *Phacelia* or *D. systyla*. The two intrusive parietal placentae completely fill the ovary. They divide the ovary into only two compartments, and the ovoid ovules develop on the adaxial surface of the placentae (Fig. 9E, F). The ovules of each compartment alternate

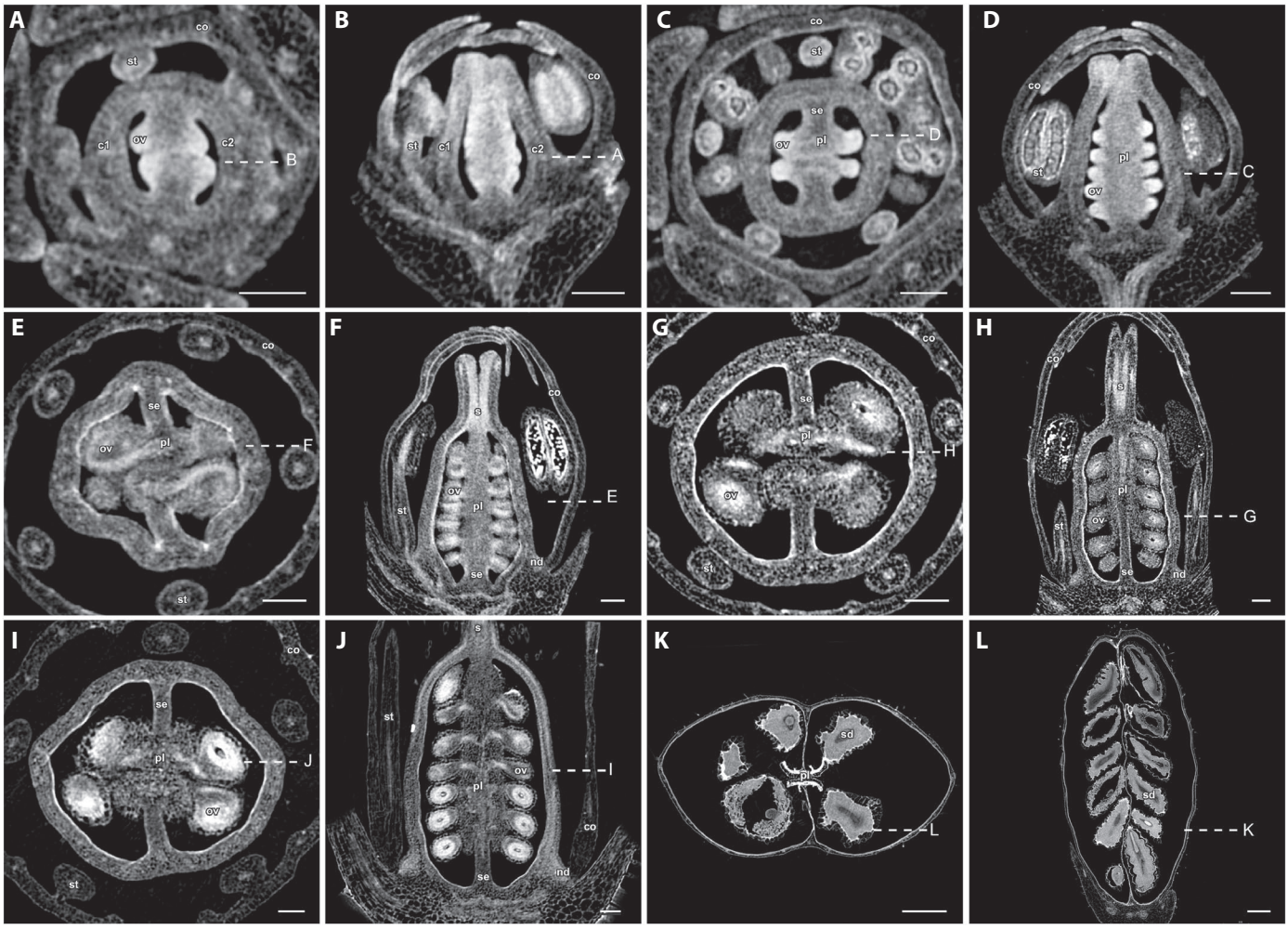

FIGURE 7. Internal development of the gynoecium and fruit in *Phacelia cumingii* based on virtual sections reconstructed from µCT scans. (A, B) Young flower with gynoecium at the stage of gynoecial cone; onset of ovules development. (A) Virtual cross section. (B) Virtual longitudinal section. (C, D) Young flowers with gynoecium at the stage of ovary formation; individual ovules become distinct. (C) Virtual cross section. (D) Virtual longitudinal section. (E–H) Pre-anthetic flowers focused on the gynoecium; ovary enlargement, style elongation, further development of ovules and placentae, development of distinct septa. (E, G) Virtual cross section. (F, H) Virtual longitudinal section. (I, J) Anthetic gynoecium. (I) Virtual cross section through the ovary, mid level. (J) Virtual longitudinal section through the ovary, within the carpels. (K, L) Mature capsule. (K) Virtual cross section through the mature capsule, mid level. (L) Virtual longitudinal section through the mature capsule. Dashed white lines with letters indicate the corresponding reconstructed sections in other panels of this figure. c1, carpel 1; c2, carpel 2; co, corolla; nd, nectary disc; ov, ovule; pl, placenta; s, style; sd, seed; se, septa; st, stamen. Bars (A–J) = 100 µm; (K, L) = 500 µm.

due to lack of space. The extent of the nectary is not morphologically distinct (Fig. 9F).

Nemophila menziesii (Fig. 9G, H) is a pluri-ovulate species. The ovary contains two large parietal placentae, and each one has two rows (ca. three to four ovules per row) of adaxially attached globose ovules (Fig. 9G, H). All ovules are located in a central compartment of the unilocular ovary. The ovules of the facing rows of each placenta alternate (Fig. 9H). The nectary tissue is located at the lower part of the ovary (Fig. 9H).

Mature fruit: SEM data

After anthesis and successful pollination, the ovary enlarges, while the style and the nectary disc wilt, but remain attached to the developing capsule. The basic ovary architecture is usually preserved in fruit. The dehiscence line becomes visible when the fruit is almost mature (Figs. 10A, 10E, 10I, 10M, 11A, 11E, 11J). The mature capsules are two-valved and loculicidally dehiscent. The studied species were either one- to four-seeded (*Phacelia tanacetifolia*, *Phacelia viscosa*, *Draperia systyla*, *Hydrophyllum virginianum*) or many-seeded (*Phacelia campanularia*, *Phacelia cumingii*, *Eucrypta chrysanthemifolia*, *Nemophila menziesii*).

Phacelia tanacetifolia (Fig. 10A–D)—The shrinking style stays attached to one of the two valves of the open capsule (Fig. 10B, C). The seeds completely fill the inner space of the capsule (Fig. 10C). Their outer surface touches the ovary wall and the adjacent seed (Fig. 10C). The inner surface of the capsule is smooth (Fig. 10D). Seeds are ovate-elliptic in outline. The outer seed-coat is moderately reticulate, and the raphal side has deep cavities (not shown).

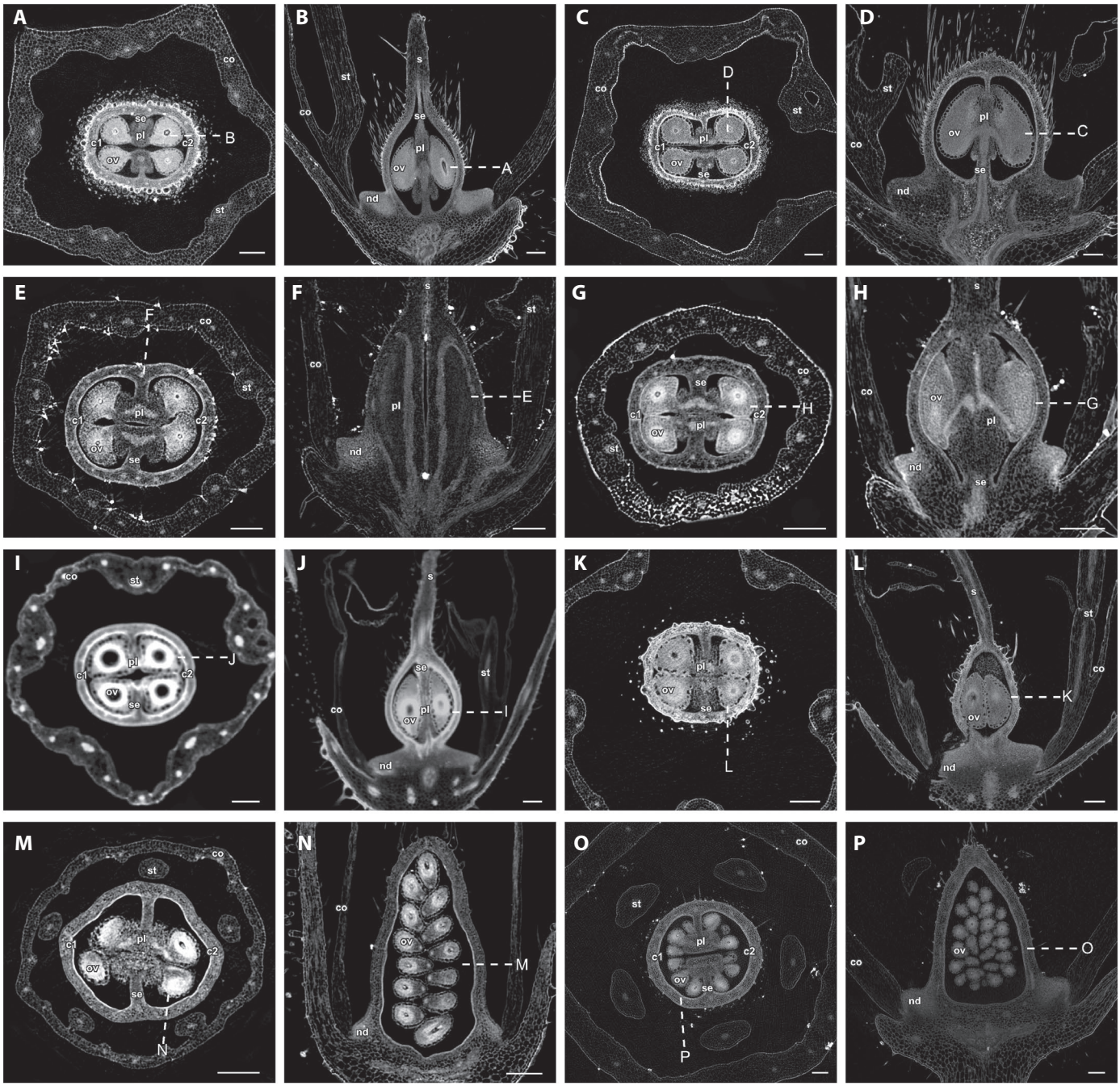

FIGURE 8. Virtual sections of anthetic flowers of eight *Phacelia* species based on µCT scans. (A–D) *Phacelia* sect. *Phacelia*. (A, B) *Phacelia secunda*. (A) Virtual cross section. (B) Virtual longitudinal section. (C, D) *Phacelia egena*. (C) Virtual cross section. (D) Virtual longitudinal section. (E–H) *Phacelia* sect. *Glandulosae*. (E, F) *Phacelia viscosa*. (E) Virtual cross section. (F) Virtual longitudinal section. (G, H) *Phacelia setigera*. (G) Virtual cross section. (H) Virtual longitudinal section. (I–L) *Phacelia* sect. *Ramosissimae*. (I, J) *Phacelia tanacetifolia*. (I) Virtual cross section. (J) Virtual longitudinal section. (K, L) *Phacelia malvifolia*. (K) Virtual cross section. (L) Virtual longitudinal section. (M, N) *Phacelia* sect. *Euglypta*; *Phacelia cumingii*. (M) Virtual cross section. (N) Virtual longitudinal section. (O, P) *Phacelia* sect. *Whitlavia*; *Phacelia campanularia*. (O) Virtual cross section. (P) Virtual longitudinal section. Dashed white lines with letters indicate the corresponding reconstructed sections in other panels of this figure. c1, carpel 1; c2, carpel 2; co, corolla; nd, nectary disc; ov, ovule; pl, placenta; s, style; se, septa; st, stamen. Bars = 200 µm.

Phacelia viscosa (Fig. 10E–H)—The inner surface of the capsule is smooth (Fig. 10G, H). The seeds do not completely fill the inner space of the capsule. The outer seed-coat has a smooth surface, and there is also a distinct ring formation on the margins (not shown). The raphal surface consists of robust globose cells (Fig. 10H).

Phacelia campanularia (Fig. 10I–L)—The ovary elongates and significantly increases in size (Fig. 10I). When the mature ovoid capsule opens, the style splits into two parts (Fig. 10J, K). Each part has a large placenta (Fig. 10L). The seeds are many and have a uniform antiraphal and raphal side, and both sides have large round pits (Fig. 10L).

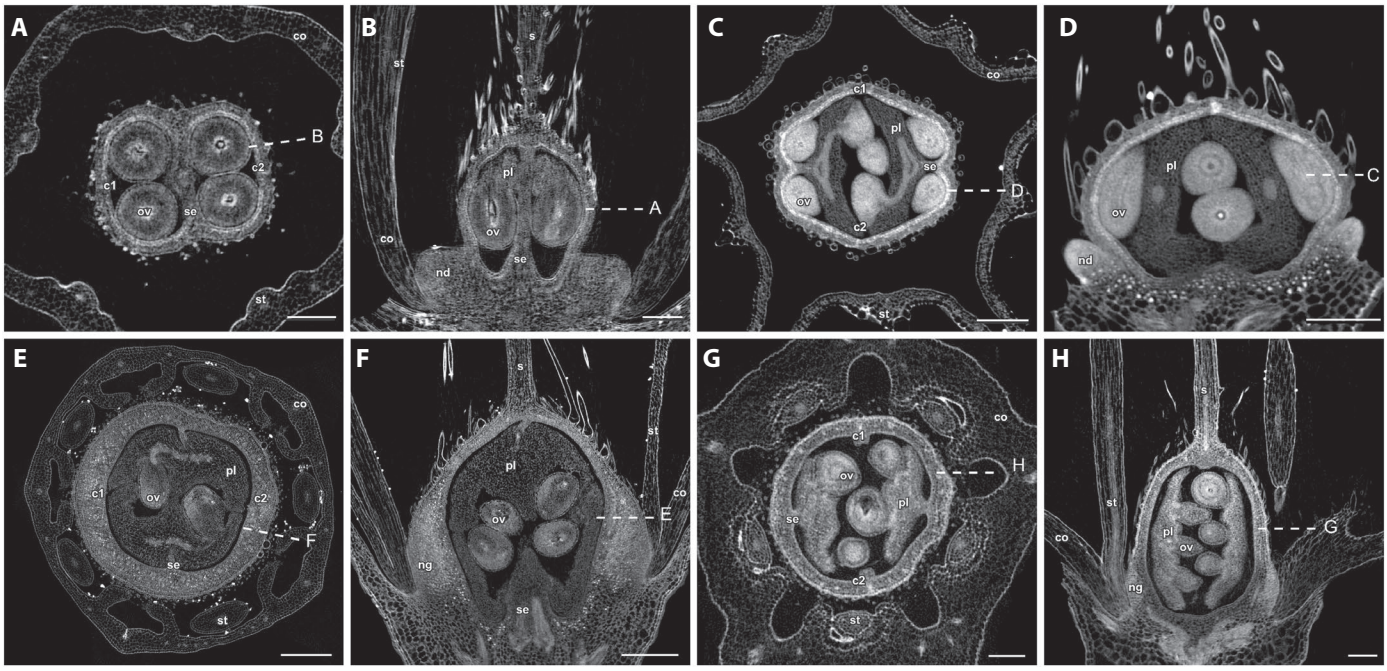

FIGURE 9. Virtual sections of anthetic flowers of *Draperia*, *Eucrypta*, *Hydrophyllum*, and *Nemophila* based on µCT scans. (A, B) Anthetic gynoecium of *Draperia systyla*. (A) Virtual cross section through the ovary, mid level. (B) Virtual longitudinal section. (C, D) Anthetic gynoecium of *Eucrypta chrysanthemifolia*. (C) Virtual cross section through the ovary, mid level. (D) Virtual longitudinal section. (E, F) Anthetic gynoecium of *Hydrophyllum virginianum*. (E) Virtual cross section through the ovary, mid level. (F) Virtual longitudinal section. (G, H) Anthetic gynoecium of *Nemophila menziesii*. (G) Virtual cross section through the ovary, mid level. (H) Virtual longitudinal section. Dashed white lines with letters indicate the corresponding reconstructed sections in other panels of this figure. c1, carpel 1; c2, carpel 2; co, corolla; nd, nectary disc; ng, nectary glands; ov, ovule; pl, placenta; s, style; se, septa; st, stamen. Bars (A–D, G, H) = 200 µm; (E, F) = 500 µm.

Phacelia cumingii (Fig. 10M–P)—The ovary wall bulges over the seeds and at the stage of the mature capsule touches the seeds (lateral side; Fig. 10M–P). The seeds are many and alternate in an individual carpel (Fig. 10N). Seeds have uniform antiraphal and raphal side, and the seed coat consists of large, almost rectangle cells, that become smaller toward the raphal side.

Draperia systyla (Fig. 11A–C)—The surface of the mature fruit is embossed. The two longitudinal lines of dehiscence are discernible when the fruit is almost mature (Fig. 11A). The loculicidal capsule dehisces from the base (Fig. 11A). The seeds are ovate-elliptic in shape (Fig. 11C). The seed-coat surface is moderately reticulate with polygonal cavities.

Eucrypta chrysanthemifolia (Fig. 11D–F)—The mature capsule opens from the lower to the upper part (Fig. 11E) and finally, one of the valves detaches (Fig. 11F). In observations of one valve of the opened capsule (Fig.11F), the layer of the large placenta that persists in fruit and the four cavities where the seeds of the central compartment were formerly attached are clearly visible. The flattened intrusive placentae result in the formation of dimorphic seeds, due to the different developmental constraints. The distal seeds, which touch the outer surface of the placenta and the carpel wall, are oblong-ovoid and wrinkled, whereas the proximal seeds, which touch the inner surface of the placenta and each other, are ellipsoid or round and smoother (not shown).

Hydrophyllum virginianum (Fig. 11G–I)—The ovary enlarges and becomes ovoid (Fig. 11G). The two longitudinal dehiscence lines are discernible in the mature fruit. The dehiscence proceeds from the upper to the lower part. The two large placentae line the fruit (Fig. 11I). Usually, two subglobose osculatory seeds are well fastened at the center of the opened capsule (Fig. 11H). The seeds have a reticulate surface, and a reduced cucullus (an appendage derived in this case from the outer epidermis of the integument and attached to the chalazal end of the mature seed) is present (not shown).

Nemophila menziesii (Fig. 11J–L)—The ovary increases significantly in size (Fig. 11J). The dried style stays attached to one valve of the dehiscent capsule (Fig. 11J). The placentae line the opened capsule (Fig. 11L). Seeds of *N. menziesii* are globose and attached to the chalazal end. A cucullus and elaiosomes are present (not shown).

Mature fruit: µCT-data

The spatial arrangement of the ovules and placentae persist in fruit, and the seeds usually have the same shape as the ovules (*P. malvifolia* [Fig. 5K, L; Appendix S4], *P. tanacetifolia*, *P. secunda*, *P. egena*), but with the notable exception of *P. setigera*. The septa are well visible in fruit. In all four-seeded species scanned, the seeds tend to gradually fill in completely the inner space of the capsule, during fruit maturation. In flowers where not all four ovules are fertilized, the mature seeds become larger, have a more rounded shape and tend to fill the empty space left by the unfertilized ovules (not shown).

Phacelia campanularia (Fig. 6K, L)—The placenta tissue does not collapse at seed maturity and fills large portions of the capsule (Fig.

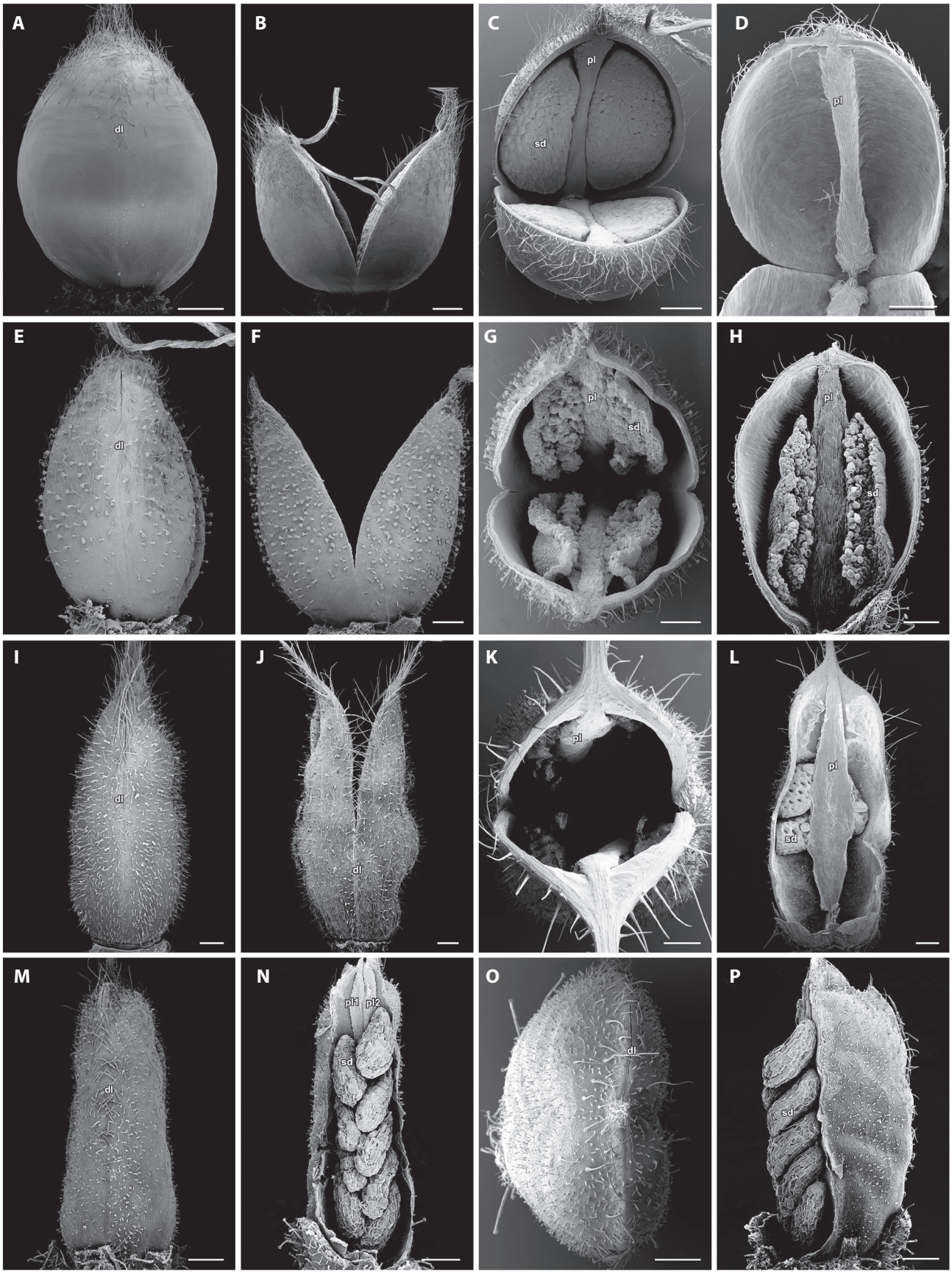
A
dl
B
C
pl
sd
D
pl
E
dl
F
G
pl
sd
H
pl
sd
I
dl
J
dl
K
pl
L
pl
sd
M
dl
N
pl1
pl2
sd
O
dl
P
sd

FIGURE 10. Mature fruits of four *Phacelia* species. (A–D) *Phacelia tanacetifolia*. (A) Outer view of a closed capsule with dehiscence line visible. (B) Outer view of an opened capsule. (C) View from above of an opened capsule with four seeds. (D) Inner view of one capsule valve; seeds were removed and placenta bundle is visible. (E–H) *Phacelia viscosa*. (E) Outer view of a closed capsule with dehiscence line visible. (F) Outer view of an opened capsule. (G) View from above of an opened capsule with four seeds. (H) Inner view of one capsule valve; two seeds and the placenta bundle are visible. (I–L) *Phacelia campanularia*. (I) Outer view of a closed capsule with dehiscence line visible. (J) Outer view of an opened capsule. (K) View from above of an opened capsule with four seeds. (L) Inner view of one capsule valve; a few seeds and the placenta bundle are visible. (M–P) *Phacelia cumingii*. (M) Outer view of a closed capsule with dehiscence line visible. (N) Inner view of a capsule; pericarp of one carpel has been removed; the two placentae touch each other; seeds alternate. (O) View from above of a closed capsule. (P) Lateral view of a capsule (looking at the line of carpel fusion); pericarp has been partially removed. dl, dehiscence line; pl, placenta (1 and 2); sd, seed. Bars = 500 μm.

6K, L). The seeds are generally uniform, but become smaller toward the base of the capsule (Fig. 6L).

Phacelia cumingii (Fig. 7K, L)—As the ovary enlarges, the fertilized ovules drastically elongate. Shortly before fruit maturity, the placenta tissue collapses after seed maturity and becomes very thin (Fig. 7K, L). The seeds in each carpel alternate and are attached to each other (Fig. 7L), but still they leave a lot of space unoccupied (Fig. 7K).

Phacelia setigera (not shown)—The shape of the ovules changes remarkably. The placentae continue to increase in size during fruit maturation, and there is limited space for the development of the seeds. The seeds at maturity are crescent-shaped, and only the hilum protrudes at the raphal side.

Ancestral character state reconstruction

Our ancestral character state reconstruction based on the *ndhF* phylogeny of Boraginales (Fig. 12) found many-seeded fruits as the likely ancestral condition in Hydrophyllaceae and the whole order. Transitions to fruits with (one to) four seeds took place at least nine times and four reversals (i.e., from four- to many-seeded fruits) were reconstructed. One transition was reconstructed in Boraginales I, for the most recent common ancestor (MRCA) of Wellstediaceae (one- to two-seeded fruits) and Boraginaceae (four-seeded fruits; Fig. 12, node i). A second transition was reconstructed for Boraginales II at the MRCA of Heliotropiaceae, Coldeniaceae, Hoplestigmataceae, Cordiaceae, and Ehretiaceae (Fig. 12, node ii). Within Hydrophyllaceae (Fig. 12, node iii), several transitions occurred. In the clade comprising *Draperia* Torr., *Tricardia* Torr. ex S.Watson, *Howellanthus* (Constance) Walden & R.Patt. and *Hesperochiron* S.Watson (hereafter DHHT clade; Fig. 12, node iv), two transitions, one in *Draperia* and one in *Howellanthus*, were reconstructed. In the Hydrophylleae clade (Fig. 12, node v), there is a transition to four-seeded fruits in the MRCA of *Hydrophyllum* L., *Nemophila* Nutt., *Pholistoma* Lilja, and *Ellisia* L. (Fig. 12, node vi). In the same clade (Hydrophylleae), a reversal to many seeds took place for the species *Nemophila menziesii*. In the large and diverse Romanzoffieae clade (Fig. 12, node vii), several transitions occurred within *Phacelia* (Fig. 12, node viii). The crown node of *Phacelia* sect. *Ramosissimae* and *Phacelia* sect. *Glandulosae* supported a transition to four-seeded capsules (Fig. 12, node ix). In *Phacelia* sect. *Ramosissimae*, only *Phacelia pauciflora* S.Watson reversed to the state of many seeds. In *Phacelia* sect. *Phacelia* (Fig. 12, node x), three transitions to four seeds were found (Fig. 12, nodes xi, xii, xiii) and two reversals back to many seeds (Fig. 12, nodes xiv, xv).

These results were largely confirmed from our ancestral character state reconstruction based on the ITS phylogeny of Hydrophyllaceae and Namaceae (Appendix S5). Many-seeded fruits were found as the likely ancestral condition in Hydrophyllaceae. Due to differences in sampling and topology, minor discrepancies were noted. In the Hydrophylleae clade, there was a transition from many to four seeds in the MRCA of *Hydrophyllum*, *Nemophila*, and *Pholistoma* (Appendix S5, node b). The results in *Phacelia* differed significantly due to low support and divergent sampling within the genus (94 taxa for ITS from which 25 are included only in this data set; 98 taxa for *ndhF* from which 26 are included only in this data set).

Seed number ranges across Hydrophyllaceae

Most of the clades which transited to four seeds (Fig. 13, nodes vi, ix, xi,) showed a conserved pattern of seed number ranges. Among the species that reversed from four back to many seeds, there was a slightly increased seed number, with the maximum values fluctuating between eight and 20. Only *Phacelia divaricata* has up to 40 seeds. Conversely, the originally multi-seeded clades showed large variation, with the maximum values of the seed number ranging between eight and 220. However, within the multi-seeded clades *P.* sect *Whitlavia*, *P.* sect. *Cosmantha*, *P.* sect *Miltitzia*, and *Euglypta*, the pattern was relatively uniform (Fig. 13).

DISCUSSION

Advances in three-dimensional (3D) approaches permit an improved visualization and a more detailed study of complex floral morphologies (Ledford, 2018; Prunet and Duncan, 2020). For ontogenetic studies, μCT offers a less laborious and nondestructive approach than anatomical serial sectioning to study the internal morphology and anatomy of flowers. Here, μCT allowed for the reconstruction of all longitudinal and cross sections of consecutive early developmental stages from a single inflorescence tip in spite of the complex inflorescence morphology of the species studied. As done in the present study, μCT should be complemented with other techniques. Here, we paired μCT with SEM to get a more comprehensive understanding of external and internal morphology and complemented these comparative results with a phylogenetic approach to gain insights into gynoecium structure and the evolution of seed numbers and morphology in Hydrophyllaceae.

The overall development of the gynoecia and fruits in Hydrophyllaceae is relatively uniform. Externally, differences are found in the position and shape of the gynoecial nectary disc, the shape of the ovary and the proportions between stylar branches and style. Internally, there are differences regarding ovule number and position in relation to the placentae, as well as the subdivision of the ovary through true and false septa. The four-ovulate species are conserved in their internal structure, and ovules and ovary appear

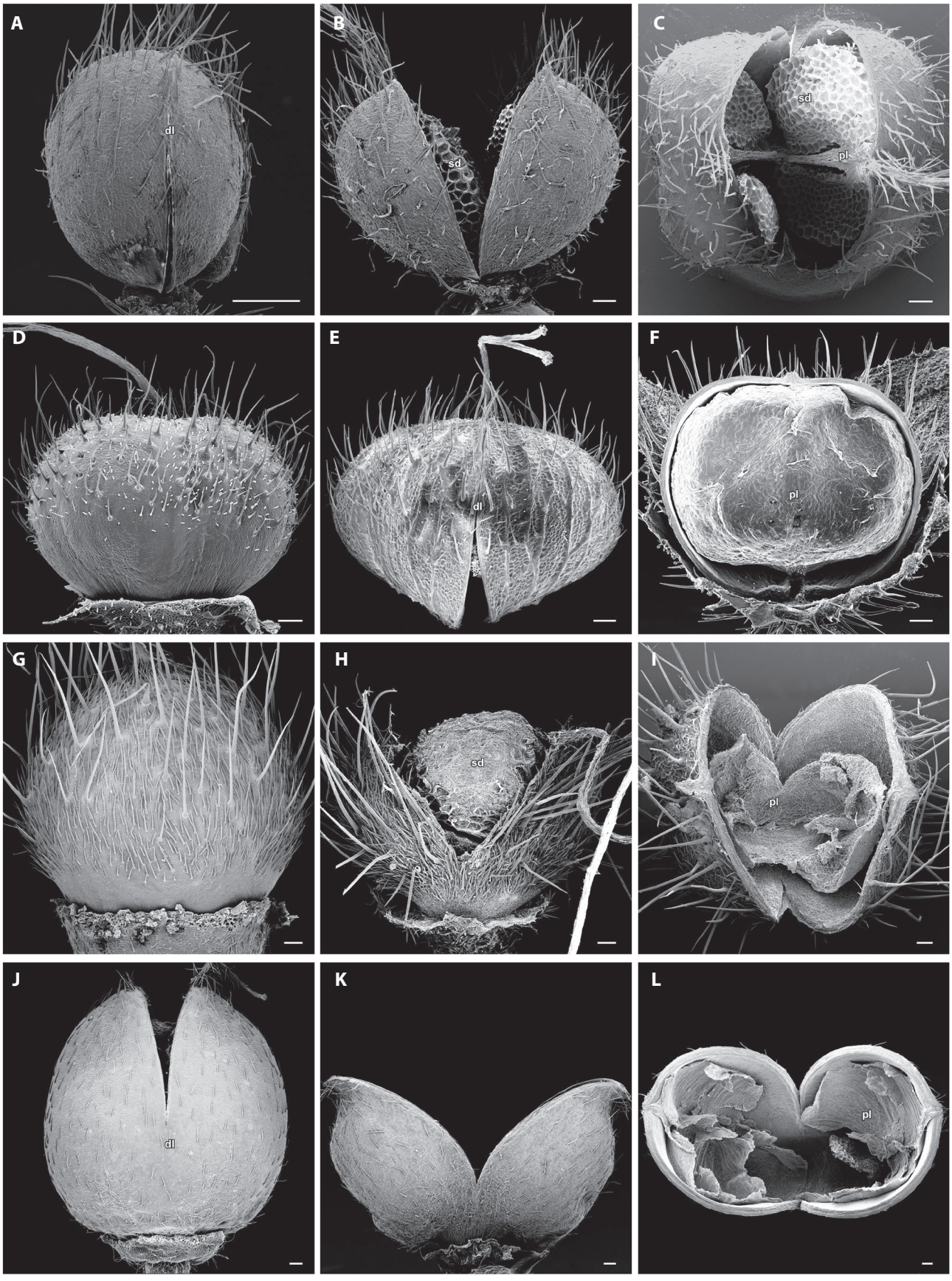
A
dl
B
sd
C
sd
pl
D
E
dl
F
pl
G
H
sd
I
pl
J
dl
K
L
pl

FIGURE 11. Mature fruits of *Draperia*, *Eucrypta*, *Hydrophyllum*, and *Nemophila*. (A–C) *Draperia systyla*. (A) Outer view of a closed capsule with dehiscence line visible. (B) Outer view of an opened capsule. (C) View from above of an opened capsule with four seeds. (D–F) *Eucrypta chysanthemifolia*. (D) Lateral view of a closed capsule (looking at the line of carpel fusion). (E) Outer view of an almost opened capsule with dehiscence line visible. (F) Inner view of one capsule valve; the placenta is lining the capsule. (G–I) *Hydrophyllum virginianum*. (G) Lateral view of a closed capsule. (H) Outer view of an opened capsule. (I) View from above of an opened capsule; the placenta is lining the capsule. (J–L) *Nemophila menziesii*. (J) Outer view of an almost opened capsule with dehiscence line visible. (K) Outer view of an opened capsule. (L) View from above of an opened capsule; the placenta is lining the capsule. dl, dehiscence line; pl, placenta; sd, seed. Bars = 200 μm.

to be tightly integrated. However, we observed differences among lineages (Romanzoffieae, Hydrophylleae, DHHT; Figs. 8, 9) mainly due to the enlarged placentae of the Hydrophylleae clade, which line or fill the ovary and lead to alternate spatial arrangement of the ovules of one layer, indicating an independent evolution of internal morphology. Based on our data set, we demonstrate that pluri-ovulate species possess several layers of ovules and two or more ovules per layer in each placenta (Table 2). Four-ovulate species have two ovules in each placenta located at one level. Reduction in ovule number results from the reduction of the number of layers and/or the number of ovule rows per placenta. These reduction mechanisms might suggest paedomorphosis, an evolutionary change in ontogeny through an alteration in the rate or timing of a developmental pathway, resulting in more derived species appearing juvenilized in comparison to their ancestors (Box and Glover, 2010). Four-ovulate species have larger ovules, which usually occupy the entire internal volume of the ovary, in comparison to the pluri-ovulate species. Full occupancy of the ovary space might thus result in the observed conservativeness of four-seededness, while the lack of spatial constraints may result in greater variation in seed number in the pluri-ovulate species. The variation might also be related to the mode of ovule insertion that we found in our sampling: The ovules develop sequentially and acropetally. This mode of development might allow for higher plasticity—ovule initiation might be terminated at any point in ovary development under resource limitation. An increase in ovule rows per placenta might have a similar effect on plasticity in ovule number. From our developmental and morphological study of Hydrophyllaceae gynoecia, it becomes apparent that the study of external features of the ovaries alone is insufficient to understand gynoecial and fruit evolution in Hydrophyllaceae and in Boraginales in general.

The study of fruit evolution in Boraginales has always been focused on the transition from dehiscent capsules to indehiscent mericarps and drupes. This transition has likely happened independently in Boraginales I and II (Weigend et al., 2013, 2014; Luebert et al., 2016). One of the underlying mechanisms is the reduction of ovule number from many to four. Our reconstruction confirms these transitions in the previously proposed positions in the Boraginales phylogeny (Fig. 12). Based on our plastid phylogeny, we reconstruct a total of at least seven reductions in seed number for Hydrophyllaceae and at least four reversals from four to many seeds, three of them within the genus *Phacelia* and one in *Nemophila*. "Four seeds" appears as quite a discrete state in the phylogeny. Conversely, exact seed number is quite variable in "many-seeded" clades, with seed numbers varying between eight and 220 even between closely related species (Fig. 13). A nonsignificant, negative correlation between seed and fruit size has been reported for *Phacelia*, indicating that larger capsules contain more and smaller seeds (Primack, 1987).

Mechanisms involved in increase of seed number have been reported for other plant groups in the asterids (e.g., Gentianaceae; Shamrov, 2018). These include an increase in placenta size and a multiplication of ovule rows per placenta, a variation of ovule size and changes of ovule orientation and arrangement (Endress, 1994; Shamrov, 2018). Our data provide further evidence for all these mechanisms and show that they are also at work in Hydrophyllaceae. We additionally observed the following mechanisms for increasing seed number per fruit: multiplication of ovule layers, locule expansion in *Nemophila menziesii*, a species that reversed from four to many seeds, and the formation of the very flattened placentae in *Eucrypta crysanthemifolia*, a likely apomorphic character. The intrusive, flattened placentae, on which ovules develop on the inner and outer surfaces, is one of the mechanisms that allowed for the increase of ovules number per layer (eight instead of four).

We have no unequivocal explanation for the variability in seed number in Hydrophyllaceae, contrasting with the high degree of conservation of four seeds across most of the order Boraginales. Variability of seed numbers in Hydrophyllaceae may be explained by the fact that capsular fruits release the seeds, and selection thus mainly acts on aspects relevant to seed dispersal and establishment. Conversely, the enclosure of the seeds in mericarps and the functional integration of the seed and fruit wall in indehiscent Boraginales is likely an evolutionary constraint limiting changes in seed number. The functional integration of mericarp and seed has been shown to be largely irreversible in other plant groups (Campanulidae, Beaulieu and Donoghue, 2013; eumalvoids, Areces-Berazain and Ackerman, 2017). There are only two instances of a reversal to many-seededness in Boraginales: mericarp multiplication in *Trigonotis* (Boraginaceae; Weigend et al., 2016) and secondary multiplication and subdivision of the carpels in the context of a highly derived fruit morphology in parastitic Lennoaceae (Yatskievych and Mason, 1986). The increase of dispersal units in Lennoaceae likely has to be considered as correlated to the transition to parasitism (as found in other parasitic plant groups: e.g., *Striga* Orobanchaceae, Press and Graves, 1995; Cytinaceae in Malvales, Nickrent, 2007; *Hydnora*, Aristolochiaceae, Bolin et al., 2018).

Dry, many-seeded, dehiscent fruits have been proposed as the ancestral condition in various flowering plant groups (Cleomoideae, Bremer and Wanntorp, 1978; Campanulidae, Beaulieu and Donoghue, 2013; Centropogonids; Lagomarsino et al., 2014; Malvaceae, Areces-Berazain and Ackerman, 2017; core Lamiids and Ericales, but not Campanuliids, Zhang et al., 2020). They are considered as the starting point of various modifications leading to subsequent fruit diversification (e.g., schizocarps, achenes). Here, we show that a seed number of four is common, but not entirely fixed in Hydrophyllaceae, whereas it is largely conserved in the rest of Boraginales, with four seeds functionally integrated into mericarps. This transition from many-seeded capsules to four-seeded schizocarps likely involves additional crucial steps such as carpel bulging (Endress, 2011) and the loss of dehiscence (Beaulieu et al.,

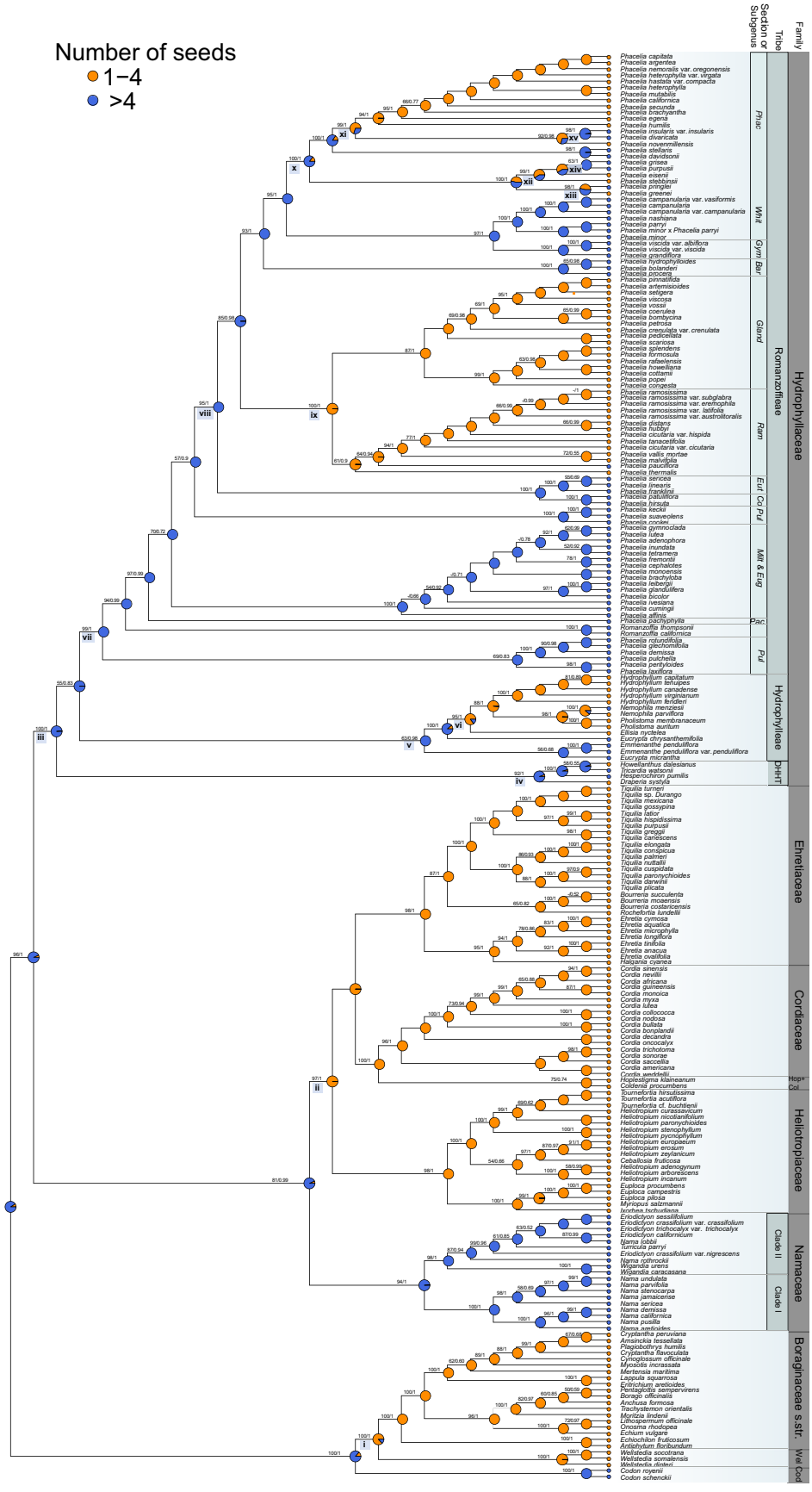
Number of seeds
1–4
>4
Family
Tribe
Section or Subgenus
Hydrophyllaceae
Romanzoffieae
Phac
Whit
Gym
Bar
Glan
Ran
Eut
Cir
Pul
Mik & Eng
Pac
Pul
Hydrophylleae
DrHT
Ehretiaceae
Cordiaceae
Hop+Cal
Heliotropiaceae
Namaceae
Clade II
Clade I
Boraginaceae s.str.
Wel
Cod

FIGURE 12. Ancestral state reconstruction of seed number evolution in Boraginales using the maximum likelihood *ndhF* tree. Key nodes (of significant clades or nodes showing transitions or reversals) are numbered (i–xv). Support values (BS/PP) are given above branches. Character scores are color-coded (orange = 1–4 seeds; blue = more than 4 seeds). Names of different taxonomic groups are displayed. *Bar*, *Baretiana*; *Co, Cosmantha*; Col, Coldeniaceae; DHHT, *Draperia* + *Howellanthus* + *Hesperochiron*+ *Tricardia* clade; *Eut*, *Eutoca*; *Gland*, *Glandulosae*; *Gym*, *Gymnobytha*; Hop, Hoplestigmataceae; *Milt & Eug*, *Miltitzia* and *Euglypta*; *Pac*, *Pachyphyllae*; *Phac*, *Phacelia*; *Pu*, *Pulchella*; *Whit*, *Whitlavia*.

2013). Similar conservation of seed number in the context of mericarp formation has also taken place in Lamiaceae. They are characterized by drupaceous or dry, indehiscent fruits separating into two two-seeded or frequently, four one-seeded mericarps (Harley et al., 2004), while their ancestor had capsular fruits (Zhang et al., 2020). Another similar case is found in Asteraceae (+ Calyceraceae), with seed number fixed to one and no reversals to many-seeded fruits, despite the fact that closely allied families (Goodeniaceae) are universally provided with many-seeded capsular fruits. Asteraceae and Lamiaceae—like both crown clades of Boraginales—have no representatives that reverted to many-seeded capsules, indicating that the functional integration of seed and fruit wall is a near-irreversible step in evolution.

CONCLUSIONS

Our data on seed numbers in capsular-fruited Hydrophyllaceae indicate that a reduction and multiplication of seed number is readily reversible as long as fruits remain dehiscent. The ontogeny of the internal ovary organization revealed at least four independently evolved developmental mechanisms (multiplication of ovule layers, multiplication of ovule rows per placenta, locule expansion, and intrusive, flattened placentae that allow for the development of ovules on the inner and outer surface) for secondarily increasing ovule number. On the other hand, the most probable mechanism for the reduction in the ovule number to four is the truncation of ovary development after the initiation

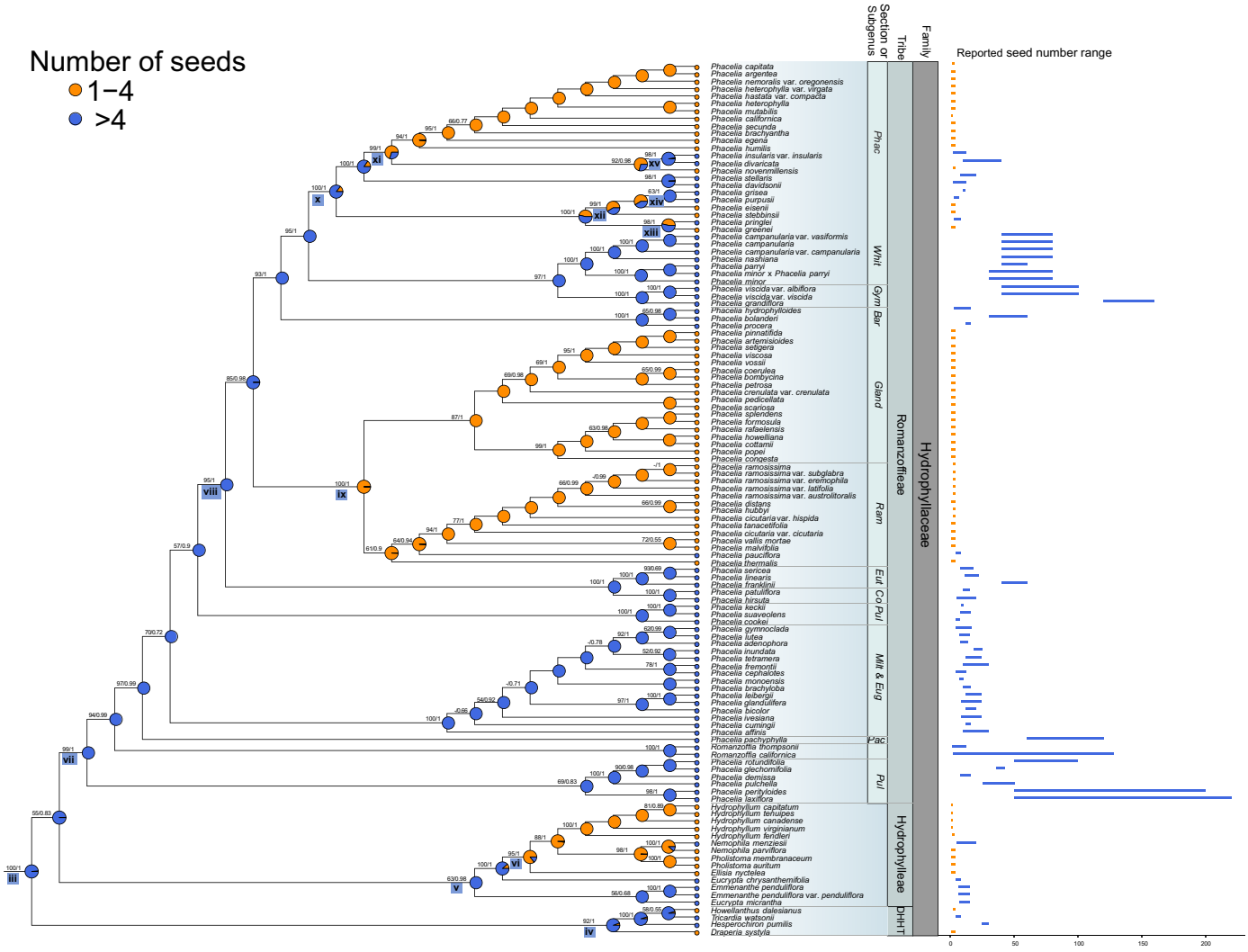

FIGURE 13. Reported seed number ranges of Hydrophyllaceae species illustrated next to the ancestral character state reconstruction. Orange bars show species with 1–4 seeds; blue bars show species with more than 4 seeds.

of the first layer of four ovules. This transition to four-ovulate ovaries appears to have happened several times independently within Hydrophyllaceae.

ACKNOWLEDGMENTS

The authors gratefully acknowledge the Bonn University Botanic Gardens for providing plant material and plant collectors T. Böhnert, A. Moreira, M. Neumann and F. Trabert. We thank Dr. Alexander Ziegler, Institut für Evolutionsbiologie und Ökologie, for the wonderful collaboration regarding the µCT scans. We thank J. Schönenberger, Y. M. Staedler, S. Pamperl, and S. Sontag for their help with the µCT in Vienna. Funding for the Skyscan 1272 µCT was provided by the Deutsche Forschungsgemeinschaft (INST 217/849-1 FUGG). We deeply appreciate the assistance of T. Joßberger and H. J. Ensikat during this study. We are grateful to Editor-in-Chief Dr. Pamela Diggle, the Associate Editor, and two anonymous reviewers for their constructive comments on an earlier version of this manuscript. Finally, we thank the Bodossaki Foundation for funding the studies of M.-A.V. in the Plant Sciences master's program at Bonn University.

AUTHOR CONTRIBUTIONS

F.L., J.J., and M.W. conceived the research idea; F.L., J.J., and M.W. designed the research; M.-A.V. performed the experiments; M.-A.V., F.L., and J.J. contributed to the data analyses; M.-A.V. performed the data visualization; M.-A.V., F.L., and J.J. drafted the manuscript, and all authors revised it.

DATA AVAILABILITY

All sequences used in this study are deposited in GenBank (Appendix S2). The alignments and the Rscript used for the ancestral character state reconstructions are available from Zenodo Repository: https://doi.org/10.5281/zenodo.4469294. The reconstructed image stacks of the scanned objects are available upon request.

SUPPORTING INFORMATION

Additional Supporting Information may be found online in the supporting information tab for this article.

APPENDIX S1. Scan settings used for x-ray microcomputed tomography.

APPENDIX S2. List of taxa, voucher information, and GenBank accessions.

APPENDIX S3. Reported numbers of seeds or ovules in Boraginales.

APPENDIX S4. Volume rendering of *Phacelia malvifolia* capsule.

APPENDIX S5. Ancestral state reconstruction of seed number evolution in Hydrophyllaceae and Namaceae using the maximum likelihood ITS tree.

LITERATURE CITED

Areces-Berazain, F., and J. D. Ackerman. 2017. Diversification and fruit evolution in eumalvoids (Malvaceae). *Botanical Journal of the Linnean Society* 184: 401–417.

Atwood, N. D. 1975. A revision of the *Phacelia Crenulatae* group (Hydrophyllaceae) for North America. *Great Basin Naturalist* 35: 127–190.

Beaulieu, J. M., and M. J. Donoghue. 2013. Fruit evolution and diversification in campanulid angiosperms. *Evolution* 67: 3132–3144.

Beaulieu, J. M., D. C. Tank, and M. J. Donoghue. 2013. A Southern Hemisphere origin for campanulid angiosperms, with traces of the break-up of Gondwana. *BMC Evolutionary Biology* 13: 80.

Berg, R. Y. 1985. Gynoecium and development of embryo sac, endosperm, and seed in *Pholistoma* (Hydrophyllaceae) relative to taxonomy. *American Journal of Botany* 72: 1775–1787.

Bolin, J. F., D. Lupton, and L. J. Musselman. 2018. *Hydnora arabica* (Aristolochiaceae), a new species from the Arabian Peninsula and a key to *Hydnora*. *Phytotaxa* 338: 99–108.

Bolmgren, K., and O. Eriksson. 2005. Fleshy fruits – origins, niche shifts, and diversification. *Oikos* 109: 255–272.

Box, M. S., and B. J. Glover. 2010. A plant developmentalist's guide to paedomorphosis: reintroducing a classic concept to a new generation. *Trends in Plant Science* 15: 241–246.

Brand, A. 1913. Hydrophyllaceae. *In* A. Engler [ed.], Das Pflanzenreich, IV, vol. 251, Heft 59. Wilhelm Engelmann, Leipzig, Germany.

Bremer, K., and H.-E. Wanntorp. 1978. Phylogenetic systematics in botany. *Taxon* 27: 317–329.

Chuang, T. I., and L. Constance. 1992. Seeds and systematics in Hydrophyllaceae: tribe Hydrophylleae. *American Journal of Botany* 79: 257–264.

Di Fulvio, T. E., M. T. Cosa, and N. Dottori. 1999. Morfología y vascularización floral de *Draperia*, *Emmenanthe*, *Hesperochiron*, *Romanzoffia* y *Tricardia* (Phacelieae, Hydrophyllaceae). *Kurtziana* 27: 187–209.

Endress, P. K. 1994. Diversity and evolutionary biology of tropical flowers. Cambridge University Press, Cambridge, USA.

Endress, P. K. 2011. Evolutionary diversification of the flowers in angiosperms. *American Journal of Botany* 98: 370–396.

Eriksson, O., and B. Bremer. 1991. Fruit characteristics, life forms, and species richness in the plant family Rubiaceae. *American Naturalist* 138: 751–761.

Gottschling, M. 2004. Floral ontogeny in *Bourreria* (Ehretiaceae, Boraginales). *Flora* 199: 409–423.

Gottschling, M., F. Luebert, H. H. Hilger, and J. S. Miller. 2014a. Molecular delimitations in the Ehretiaceae (Boraginales). *Molecular Phylogenetics and Evolution* 72: 1–6.

Gottschling, M., S. Nagelmüller, and H. H. Hilger. 2014b. Generative ontogeny in *Tiquilia* (Ehretiaceae: Boraginales) and phylogenetic implications. *Biological Journal of the Linnean Society* 112: 520–534.

Harley, R. M., S. Atkins, A. L. Budantsev, P. D. Cantino, B. J. Conn, R. Grayer, M. M. Harley, et al. 2004. Labiatae. *In* J. W. Kadereit [ed.], Families and genera of vascular plants, vol. VII, 167–275. Springer, Heidelberg, Germany.

Hilger, H. H. 1992. Morphology of *Heliotropium* (Boraginaceae) dispersal units. *Botanica Acta* 105: 387–393.

Hilger, H. H. 1985. Ontogenie, Morphologie und systematische Bedeutung geflugelter und glochidientragender Cynoglosseae- und Eritricheae-Früchte (Boraginaceae). *Botanische Jahrbücher für Systematik, Pflanzengeschichte und Pflanzengeographie* 105: 323–378.

Hofmann, M. 1999. Flower and fruit development in the genus *Phacelia* (Phacelieae, Hydrophyllaceae): characters of systematic value. *Systematics and Geography of Plants* 68: 203–212.

Hofmann, M., G. K. Walden, H. H. Hilger, and M. Weigend. 2016. Hydrophyllaceae. *In* J. W. Kadereit and V. Bittrich [eds.], Families and genera of vascular plants, vol. XIV, 221–238. Springer, Heidelberg, Germany.

Jeiter, J., F. Danisch, and H. H. Hilger. 2016. Polymery and nectary chambers in *Codon* (Codonaceae): flower and fruit development in a small, capsule-bearing family of Boraginales. *Flora* 220: 94–102.

Jeiter, J., Y. M. Staedler, J. Schönenberger, M. Weigend, and F. Luebert. 2018. Gynoecium and fruit development in *Heliotropium* Sect. *Heliothamnus* (Heliotropiaceae). *International Journal of Plant Sciences* 179: 275–286.

Jeiter, J., and M. Weigend. 2018. Simple scales make complex compartments: ontogeny and morphology of stamen–corolla tube modifications in Hydrophyllaceae (Boraginales). *Biological Journal of the Linnean Society* 125: 802–820.

Jepson, W. L., and J. C. Hickman. 1993. The Jepson manual: higher plants of California. University of California Press, Berkeley, CA, USA.

Lagomarsino, L. P., A. Antonelli, N. Muchhala, A. Timmermann, S. Mathews, and C. C. Davis. 2014. Phylogeny, classification, and fruit evolution of the species-rich Neotropical bellflowers (Campanulaceae: Lobelioideae). *American Journal of Botany* 101: 2097–2112.

Ledford, H. 2018. The lost art of looking at plants. *Nature* 553: 396–398.

Lorts, C. M., T. Briggeman, and T. Sang. 2008. Evolution of fruit types and seed dispersal: a phylogenetic and ecological snapshot. *Journal of Systematics and Evolution* 46: 396–404.

Luebert, F., L. Cecchi, M. W. Frohlich, M. Gottschling, C. M. Guilliams, K. E. Hasenstab-Lehman, H. H. Hilger, et al. 2016. Familial classification of the Boraginales. *Taxon* 65: 502–522.

Nickrent, D. L. 2007. Cytinaceae are sister to Muntingiaceae (Malvales). *Taxon* 56: 1129–1135.

Paradis, E., and K. Schliep. 2019. ape 5.0: an environment for modern phylogenetics and evolutionary analyses in R. *Bioinformatics* 35: 526–528.

Patterson, T. B., and T. J. Givnish. 2002. Phylogeny, concerted convergence, and phylogenetic niche conservatism in the core Liliales: Insights from *rbcL* and *ndhF* sequence data. *Evolution* 56: 233–252.

Payer, J.-B. 1857. Traité d'organogénie camparée de la fleur. Masson, Paris, France.

Press, M., and J. Graves [eds.]. 1995. Parasitic plants. Chapman & Hall, London, UK.

Primack, R. B. 1987. Relationships among flowers, fruits, and seeds. *Annual Review of Ecology and Systematics* 18: 409–430.

Prunet, N., and K. Duncan. 2020. Imaging flowers: a guide to current microscopy and tomography techniques to study flower development. *Journal of Experimental Botany* 71: 2898–2909.

Revell, L. J. 2012. phytools: an R package for phylogenetic comparative biology (and other things). *Methods in Ecology and Evolution* 3: 217–223.

Schindelin, J., I. Arganda-Carreras, E. Frise, V. Kaynig, M. Longair, T. Pietzsch, S. Preibisch, et al. 2012. Fiji: an open-source platform for biological-image analysis. *Nature Methods* 9: 676–682.

Schneider, A. C., T. Braukmann, A. Banerjee, and S. Stefanović. 2018. Convergent plastome evolution and gene loss in holoparasitic Lennoaceae. *Genome Biology and Evolution* 10: 2663–2670.

Sher, E. M., and A. Weber. 2009. Floral ontogeny of Oleaceae and its systematic implications. *International Journal of Plant Sciences* 170: 845–859.

Shamrov, I. I. 2018. Diversity and typification of ovules in flowering plants. *Wulfenia* 25: 81–109.

Spjut, R. W. 1994. A systematic treatment of fruit types. New York Botanical Garden, Bronx, NY, USA.

Staedler, Y. M., D. Masson, and J. Schönenberger. 2013. Plant tissues in 3D via x-ray tomography: Simple contrasting methods allow high resolution imaging. *PLoS One* 8: e75295.

Stull, G. W., R. D. de Stefano, D. E. Soltis, and P. S. Soltis. 2015. Resolving basal lamiid phylogeny and the circumscription of Icacinaceae with a plastome-scale data set. *American Journal of Botany* 102: 1794–1813.

Vasile, M.-A., J. Jeiter, M. Weigend, and F. Luebert. 2020. Phylogeny and historical biogeography of Hydrophyllaceae and Namaceae, with a special reference to *Phacelia* and *Wigandia*. *Systematics and Biodiversity* 18: 757–770.

Walden, G. K., and R. Patterson. 2012. Nomenclature of subdivisions within *Phacelia* (Boraginaceae: Hydrophylloideae). *Madroño* 59: 211–222.

Weigend, M., F. Luebert, M. Gottschling, T. L. P. Couvreur, H. H. Hilger, and J. S. Miller. 2014. From capsules to nutlets—phylogenetic relationships in the Boraginales. *Cladistics* 30: 508–518.

Weigend, M., F. Luebert, F. Selvi, G. Brokamp, and H. H. Hilger. 2013. Multiple origins for Hound's tongues (*Cynoglossum* L.) and Navel seeds (*Omphalodes* Mill.)—the phylogeny of the borage family (Boraginaceae s.str.). *Molecular Phylogenetics and Evolution* 68: 604–618.

Weigend, M., F. Selvi, D. C. Thomas, and H. H. Hilger. 2016. Boraginaceae. *In* J. W. Kadereit and V. Bittrich [eds.], Families and genera of vascular plants, vol. XIV, 41–102. Springer, Heidelberg, Germany.

Yatskievych, G., and C. T. Mason. 1986. A revision of the Lennoaceae. *Systematic Botany* 11: 531–548.

Zhang, C., T. Zhang, F. Luebert, Y. Xiang, Y. Hu, M. Rees, M. W. Frohlich, et al. 2020. Asterid phylogenomics/phylotranscriptomics uncover morphological evolutionary histories and support phylogenetic placement for numerous whole genome duplications. *Molecular Biology and Evolution* 37: 3188–3210.